JOURNAL OF AGRICULTURAL ENGINEERING AND TECHNOLOGY (JAET)

EDITORIAL BOARD

Editor-In-Chief
Professor A. P. Onwualu
Raw Materials Research and Development Council (RMRDC)
Plot 427 Aguiyi Ironsi Street, Maitama District, PMB 232 Garki, Abuja, Nigeria.
E-mail: ponwualu@yahoo.com Phone: 08037432497

Dr. B. Umar ï Editor, Power and Machinery
Agricultural Engineering Department, University of Maiduguri, Maiduguri, Nigeria.
E-mail: bobboiumar@yahoo.co.uk Phone: 08023825894

Professor A. A. Olufayo ï Editor, Soil and Water Engineering
Agricultural Engineering Department, Federal University of Technology, Akure, Nigeria.
E-mail: ayo_olufayo@yahoo.com Phone: 08034708846

Professor O. O. Babatunde ï Editor, Post Harvest Technology
Agricultural Engineering Department, University of Ilorin, Ilorin, Nigeria.
E-mail: oludare_babatunde@yahoo.com Phone: 08033776491

Professor A. Ajisegiri ï Editor, Food Engineering
Agricultural Engineering Department, Federal University of Technology, Minna, Nigeria.
E-mail: ajisegiri@yahoo.com Phone: 08033805960

Dr. A. El-Okene ï Editor, Structures and Environmental Control Engineering
Agricultural Engineering Department, Ahmadu Bello University, Zaria, Nigeria.
E-mail: abdullahielokene@yahoo.com Phone: 08023633464

Dr. D. S. Zibokere ï Editor, Environmental Engineering
Agric. and Environmental Engineering Dept., Niger Delta University, Wilberforce Island, Yenegoa.
E-mail: zibokere@yahoo.co.uk Phone: 08037079321

Dr. C. C. Mbajiorgu ï Editor, Emerging Technologies
Agricultural Engineering Department, University of Nigeria, Nsukka, Nigeria.
E-mail: const.c.mbajiorgu@talk21.com Phone: 08037786610

Dr (Mrs) Z. S. Osunde ï Business Manager
Agricultural Engineering Department, Federal University of Technology, Minna, Nigeria.
E-mail: zinashdo@yahoo.com Phone: 08034537068

Mr. Y. Kasali ï Business Manager
National Centre for Agricultural Mechanization, PMB 1525, Ilorin, Nigeria.
E-mail: ncam@skannet.com Phone: 08033964055

Mr. J. C. Adama – Editorial Assistant
Federal Department of Rural Development, 4 Onitsha Rd., Enugu, Nigeria.
E-mail: chuwukuma2001@yahoo.com Phone: 08052806052

Mr. B. O. Ugwuishiwu – Editorial Assistant
Agricultural Engineering Department, University of Nigeria, Nsukka, Nigeria
E-mail: ugwuishiwubo@yahoo.com Phone: 08043119327

Aims and Scope

The main aim of the Journal of Agricultural Engineering and Technology (JAET) is to provide a medium for dissemination of high quality Technical and Scientific information emanating from research on Engineering for Agriculture. This, it is hoped will encourage researchers and engineers in the area to continue to develop cutting edge technologies for solving the numerous problems facing agriculture in the third world in particular and the world in general.

The Journal publishes original research papers, review articles, technical notes and book reviews in Agricultural Engineering and related subjects. Key areas covered by the journal are: Agricultural Power and Machinery; Agricultural Process Engineering; Food Engineering; Post-Harvest Engineering; Soil and Water Engineering; Environmental Engineering; Agricultural Structures and Environmental Control; Waste Management; Aquacultural Engineering; Animal Production Engineering and the Emerging Technology Areas of Information and Communications Technology (ICT) Applications, Computer Based Simulation, Instrumentation and Process Control, CAD/CAM Systems, Biotechnology, Biological Engineering, Biosystems Engineering, Bioresources Engineering, Nanotechnology and Renewable Energy. The journal also considers relevant manuscripts from related disciplines such as other fields of Engineering, Food Science and Technology, Physical Sciences, Agriculture and Environmental Sciences.

The journal is published by the Nigerian Institution of Agricultural Engineers (NIAE), A Division of Nigerian Society of Engineers (NSE). The Editorial Board and NIAE wish to make it clear that statements or views expressed in papers published in this journal are those of the authors and no responsibility is assumed for the accuracy of such statements or views. In the interest of factual recording, occasional reference to manufacturers, trade names and proprietary products may be inevitable. No endorsement of a named product is intended nor is any criticism implied of similar products that are not mentioned.

Submission of an article for publication implies that it has not been previously published and is not being considered for publication elsewhere. The journalôs peer review policy demands that at least two reviewers give positive recommendations before the paper is accepted for publication. Prospective authors are advised to consult the Guide for Authors which is available in each volume of the journal. Four copies of the manuscript and processing fee should be sent to:

The Editor-In-Chief
Journal of Agricultural Engineering and Technology (JAET)
Ă The Editorial Office
National Centre for Agricultural Mechanization (NCAM)
P.M.B. 1525
Ilorin, Kwara State, Nigeria.

Papers can also be submitted directly to the Editor-In-Chief or any of the Sectional Editors. Those who have access to the internet can submit electronically as an attached file in MS Word to jaetniae@yahoo.com. All correspondence with respect to status of manuscript should be sent to the E-mail address above.

CONTENTS

Design and Operating Effects of Parameters on Draught of Model Chisel Furrowers in an Artificial Soil. **E. Mamman and K. C. Oni.** **4-17**

Development and Preliminary Testing of Metering Equipment for Mechanized Yam Sett Planting. **O. B. Aluko and O. A. Koya.** **18-26**

An Experimental Mechanical Cassava Tuber Peeling Machine. **D. A. Adetan, L. O. Adekoya, O. B. Aluko and G. A. Makanjuola** **27-34**

Some Physical Properties of Groundnuts (Arachis hypogea L). **A. F. Alonge and T. A. Adegbulugbe.** **35-41**

Development and Performance Evaluation of a Poultry Mixer. **L. Gbadamosi and S. A. Magaji.** **42-47**

Modeling the Changes in Size of Air-Borne Liquid Spray Droplets in Windy and Still Air Conditions. **S. I. Oluka, C. O. Akubuo and E. U. Odigboh** **48- 57**

Technologies for Extraction of Oil from Oil-Bearing Agricultural Products: A Review. **A. Ibrahim and A. P. Onwualu.** **58-70**

Component Design of a 187/kg/hr Low-Cost Extrusion Cooker for Full Fat Soya Meal. **C. U. Orji.** **71-82**

Design, Construction and Performance Evaluation of a Cowpea Thresher. **A. S. Ogunlowo and S. R. Bello** **83-89**

On the Value of Sthort-term Weather Forecasts in Scheduling Supplemental Irrigation Of Potatoes in the United Kingdom. **C. J. Ejieji, J. W. Gowing**. 9**0-105**

Hydraulic Modeling of Begeman Gate for Effective Water Management System in HVIP, Nigeria. **M. K. Othman, X. Litrico, J. P. Boume and S. Z. Abubakar** **106-116**

Instructions **117-119**

DESIGN AND OPERATING EFFECTS OF PARAMETERS ON DRAUGHT OF MODEL CHISEL FURROWERS IN AN ARTIFICIAL SOIL

E. Mamman[1] and K. C. Oni [2]
[1]Department of Agricultural Engineering, P.M.B. 1069, University of Maiduguri, Borno State, Nigeria, E-mail: mamman2002ng@yahoo.com
[2]Director, National Centre for Agricultural Mechanization, P.M.B. 1525, Ilorin, Kwara State, Nigeria

ABSTRACT

A study was conducted to determine the effects of design and operating parameters on the draught of model chisel furrowers in an artificial soil in a laboratory soil bin. The design parameters considered were slide and nose angles while operating parameters were soil depth and tool travel speed. The effects of the interactions of depth and speed on slide and nose angles were evaluated. The influences of depth and speed on the interactions of slide and nose angles were also determined. Results showed that draught increased with increases in depth, speed, slide and nose angles. Soil depth gave draught values that were slightly higher than that of tool speed. The effect of depth on the interactions of slide and nose angles resulted in higher draught than with speed. The slight differences recorded in draught of the model tools showed that the tool design parameters were a suitable combination and the tools could perform well in a good soil if depth and speed are carefully selected.

KEYWORDS: Chisel furrower, draught, soil bin, artificial soil, slide angle, nose angle.

1. INTRODUCTION

The design of tillage tools to accomplish different jobs is a very complex engineering work. This is based on the fact that different crops require different soil preparations. Different soil conditions also require different tillage operations. Shape and size are usually the first parameters to be considered in the design of any tillage tool. The shape influences the pattern of soil movement and final soil conditions while the size determines the power required to pull the tool through the soil. Although the designer can control tool shape and size, tools cannot perform optimally without proper combination and orientation of the tool design parameters. Tillage tools of different shapes and sizes have been designed and constructed for the purpose of soil manipulation. One of the most important performance criteria in tillage tool design is the force needed to pull the tool through a given soil (Gill and Vanden-Berg, 1967). Several researchers (Bukhari et al., 1990; Harrison and Bai, 1990; Oni et al., 1992; Biswas et al., 1993; Salokhe and Pathak, 1993; Hann and Giessibl, 1998; Onwualu and Watts, 1998; Shrestha et al., 2001) have investigated the relationships between tool geometry, tool travel speed and depth of tool engagement, soil failure pattern and volume of soil upheaval. The results reported by each of these researchers varied with tool geometry, operational parameters and soil conditions at the time of the experiments.

Shirin et al. (1993) evaluated the effects of disc and working parameters on the performance of a disc plough in a clay soil in the field. Experiments were conducted at disc angles of 40°, 45° and 50°; tilt angles of 17°, 20° and 23°, and average forward speeds of 3, 4 and 5 km/h. They reported that at 17° tilt and 45° disc angles, the specific draught decreased with an increase in soil moisture content for all the ploughing speeds. Draught decreased when disc angle was increased from 40° to 45°. There was a sharp increase in draught when the disc angle was changed from 45° to 50° in all cases. Increases in disc angle increased disc penetration and the width of cut. At all disc angles and speeds, there was a marked decrease in specific draught with an increase in tilt angle.

Fielke (1996) studied the effect of the cutting edge geometry of tillage implements on tillage forces, soil failure and soil movement below the tillage depth in the field and in a laboratory soil bin. He used experimental sweeps that were standardized with 400 mm width; 32 mm lift height, 10º rake angle and 70º sweep angle. He reported that increasing the speed of operation consistently increased the draught but had little effect on the vertical force. An increase in cutting edge height increased the forward and downward movement of soil at the cutting edge, and an increasing draught and vertically

upward forces accompanied this. The sharp cutting edge of the tillage tool minimized the draught and vertically upward forces and it also gave a minimum soil disturbance below the tillage depth. Mckyes and Maswaure (1997) evaluated the effects of the geometric parameters of flat tillage tools on their draught, cutting efficiency and loosening of a moist clay soil. They observed increases in draught with width, depth and rake angle of the tools. Alï Suhaibani and Al- Janobi (1997) investigated the effects of speed and depth on the draught of a chisel plough, an offset disk harrow, a mouldboard plough and a disk plough on a sandy loam soil in the field. The authors observed a significant increase in draught for all the implements with an increase in depth. The specific draughts of the four tillage implements were also affected significantly by speed and depth.

Mouazen and Nemenyi (1999) estimated the draught and vertical forces, soil deformation and normal pressure distribution on four geometrically similar subsoilers using the finite element method. The four subsoilers studied have a combination of a vertical shank with 15°, 23° and 31° inclined chisels, and a 75° rake angle shank with 15° inclined chisel. They reported that a subsoiler with a shank angle of 75° and a chisel angle of 15° had the least draught. Manian et al. (2000) conducted studies in a soil bin containing black clay loam and sand in order to assess the draught, vertical and lateral components of reaction in discs at different moisture levels. The variables used were disc angle (40, 44 and 48º), tilt angle (16, 20 and 24º), disc diameter (51, 56 and 61 cm) and forward speed (4, 7 and 10 km/h). Soil moisture content, speed and disc diameter affected the draught, vertical and lateral components of reaction in both soils at varying degrees. The 16º tilt angle setting resulted in lower draught and vertical reaction components as compared to the 24º and 30º settings. Disc angles set at 44º gave minimum draught than at 40º and 48º. The vertical reaction component decreased as the disc angle increased.

Natsis et al. (2002) investigated the influence of foreploughshare and disc coulter on tillage quality and tractor fuel consumption in a clay soil in the field. The treatments consisted of tillage with mouldboard plough equipped with both disk coulter and foreploughshare; tillage with mouldboard plough equipped with foreploughshare without disk coulter, and tillage with mouldboard plough but without disk coulter or foreploughshare. The authors reported that tillage with no foreploughshare or disk coulter produced the least soil draught while tillage with foreploughshare and no disk coulter gave the highest soil draught. Tillage with disk coulter reduced both soil draught and tractor fuel consumption. Although tillage with disk coulter and foreploughshare did not give the least soil draught, the best tillage quality was obtained at this treatment.

Despite the fact that several works have been done on the effects of design and operating parameters on numerous model tools, none was on model chisel furrowers. The objective of this study was therefore to determine the effects of design and operating parameters on the draught of model chisel furrowers in an artificial soil.

2. MATERIALS AND METHODS

The soil bin facility used for this experimental study was located in the Tillage and Traction laboratory in the Department of Agricultural Engineering, University of Ilorin. The soil bin was 5.6 m long, 0.44 m wide and 0.58 m deep. The transmission from a single-axle tractor was used as source of power for soil processing and tool carriage. The carriage (Fig. 1) was equipped with a rotary tiller, soil leveller, roller compactor, tool bar frame and tool bar. The details of the design and construction of the soil bin and the carriage accessories were presented by Mamman (2002). The rotary tiller was used for soil pulverization after each test run. The roller compactor was used to compact the pulverized soil in the soil bin to a uniform density. The tool bar carries the model tool and the transducer. A 3.73 kW, three-phase electric motor served as the prime mover for the carriage and the rotary tiller.

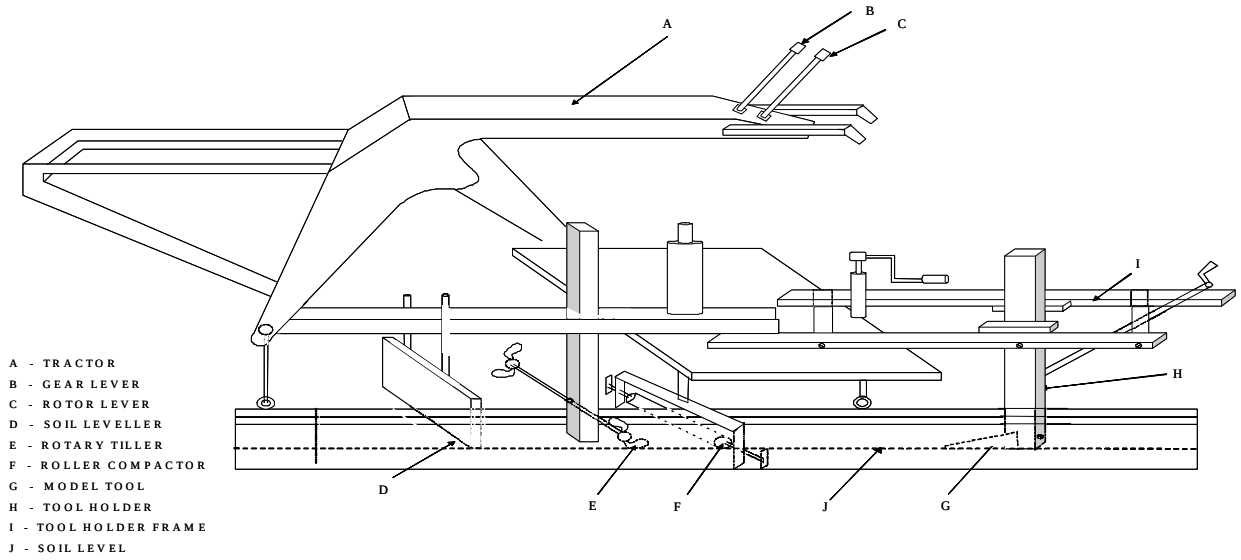


Fig.1: Schematics of a single-axle tractor showing soil processing carriage and model tool arrangements in the soil bin.

The transducer used for measuring the draught of the model tools consisted of two electrical resistance strain gages, two-140q fixed resistors and 5V power supply. One of the strain gages was mounted on one face of the tool bar in direction of travel (tension) and the other one was mounted on the opposite face of the tool bar (compression). The transducer was connected to a Wheatstone bridge. The Wheatstone bridge was connected to an amplifier, which was in turn connected to an S-T plotter. Details of the design and construction of the transducer and amplifier was presented by Mamman (2002).

The model tools were intended to create furrows in a vertisol (Typic Pellustert) for dry season sorghum (Masakwa) seedling transplanting. But because of the difficulty of getting workable moisture content, the soil was composed into an artificial soil by mixing with hydraulic transmission oil (Azolla 68 ZS). Particle size analysis of the original vertisol gave 5% sand, 35% silt and 60% clay (Ohu et al., 2001). The strength properties of the artificial soil were determined for cohesion (3.66 kPa), adhesion (3.90 kPa), soil angle of internal friction (4.17°) and soil-metal friction angle (22°).

Thirty-six geometrically similar model chisel furrowers were designed and fabricated for the study. The model tool design parameters were cutting edge height (H), slide angle (ϭ), nose angle (ɔ), width (W) and height (h). All tools were 150 mm long and the cutting edge of each was 1 mm thick. The width and height of each model tool was proportional to its nose and slide angles, respectively. The geometric parameters of the model tools considered in this report were slide and nose angles. The slide angles used were 5, 10, 15 and 20° and the nose angles were 10, 20 and 30°. The operating parameters used for the investigation were soil depth and tool travel speed. Soil depths were 2.5, 5, 7.5 and 10 cm while tool speeds were 2, 5, 10 and 15 cm/s.

A 3x3x4x4x4 (3 levels each of cutting edge height and nose angle, and 4 levels each of slide angle, speed and depth) full factorial statistical design was used for data collection. The experiments were replicated two times. Analysis of variance of the mean values of draught was carried out using a statistical package; Genstat 5 and Least Significant Difference (LSD) tool was used to test the level of significance. The mean values of draught that were statistically significant were used for the interpretation of the results. The effects of the interaction of depth and speed on slide and nose angles and the effects of the interactions of slide and nose angles on draught as affected by depth and speed were reported.

3. RESULTS AND DISCUSSION

Figures 2-5 illustrate the response of draught of model tools to changes in slide angle, tillage depth and tool travel speed. At each level of speed of operation, draught increased with increases in slide angle and tillage depth. For all slide angles and tillage depths, draught increased with increases in tool travel speed. At a tool travel speed of 2 cm/s and tillage depth of 2.5 cm, a mean draught of 76.70 N and 117.64 N were recorded at 5º and 20º slide angles, respectively. For the same tool speed (2 cm/s) and tillage depth of 10 cm, a mean draught of 118.32 N and 156.89 N were obtained at 5º and 20º slide angles, respectively. At the highest tool speed considered in the study (15 cm/s) and at tillage depth of 2.5 cm, a mean draught of 122.83 N was recorded at 5º slide angle and 154.04 N was obtained at 20º slide angle. For the same tool speed (15 cm/s) and tillage depth of 10 cm, a mean draught of 159.34 N and 188.35 N were obtained at 5º and 20º slide angles, respectively.

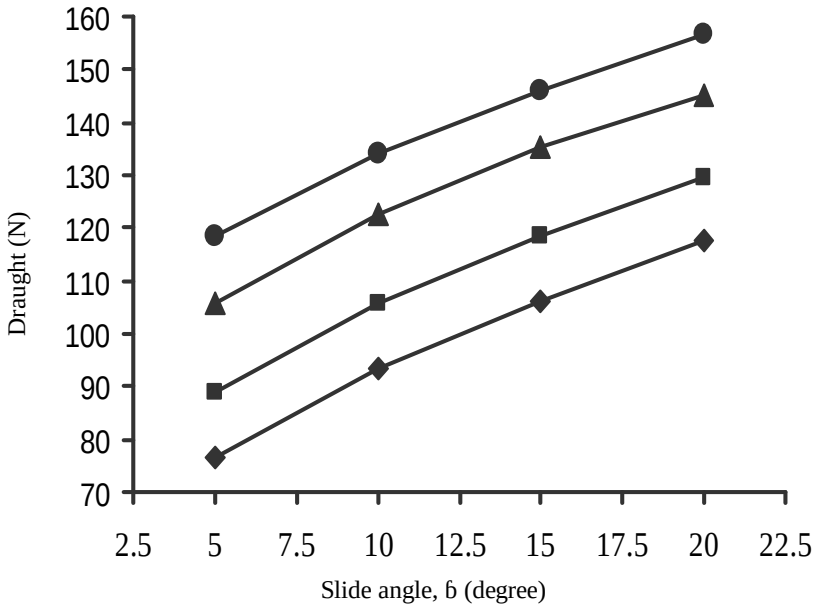


Fig. 2: Influence of slide angle and depth on draught at a speed of 2 cm/s: d=depth; d_1= 2 cm; d_2 =5 cm; d_3=7.5 cm; d_4=10 cm

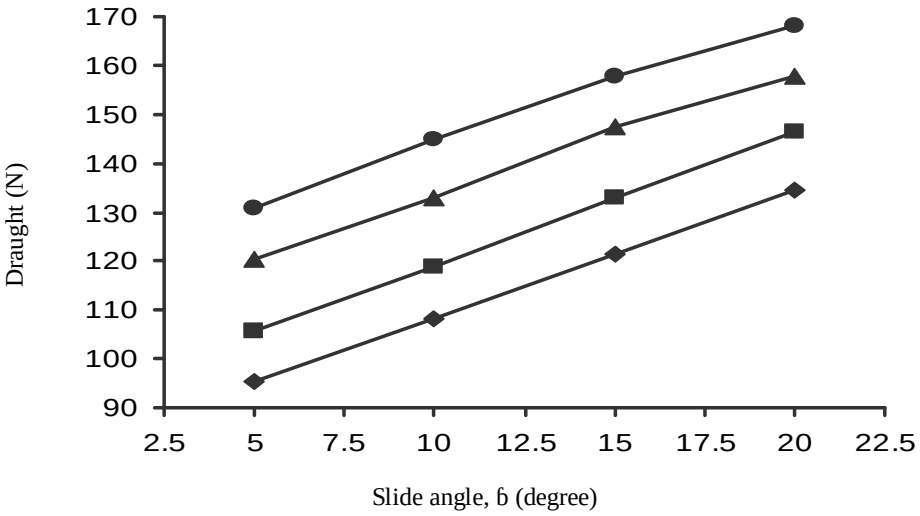


Fig. 3: Influence of slide angle and depth on draught at a speed of 5 cm/s: d=depth; d_1= 2 cm; d_2 =5 cm; d_3=7.5 cm; d_4=10 cm

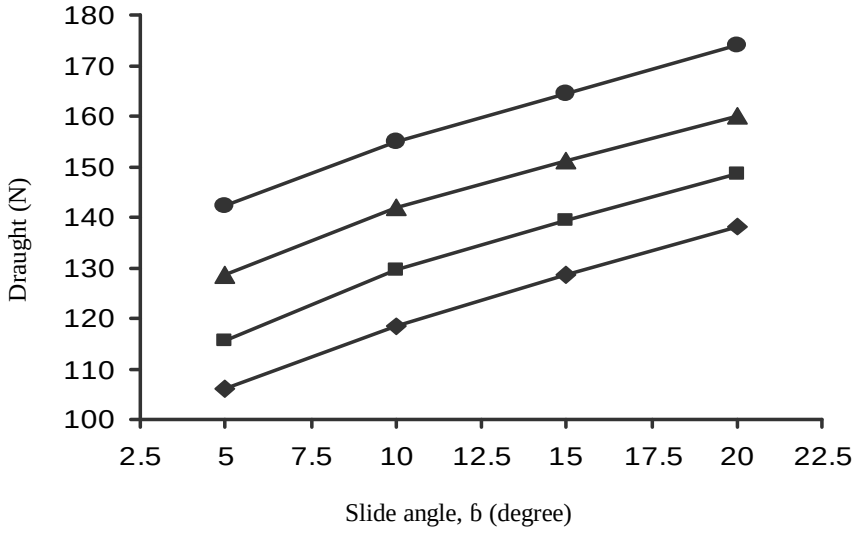


Fig. 4: Influence of slide angle and depth on draught at a speed of 10 cm/s: d=depth; d_1= 2 cm; d_2 =5 cm; d_3=7.5 cm; d_4=10 cm

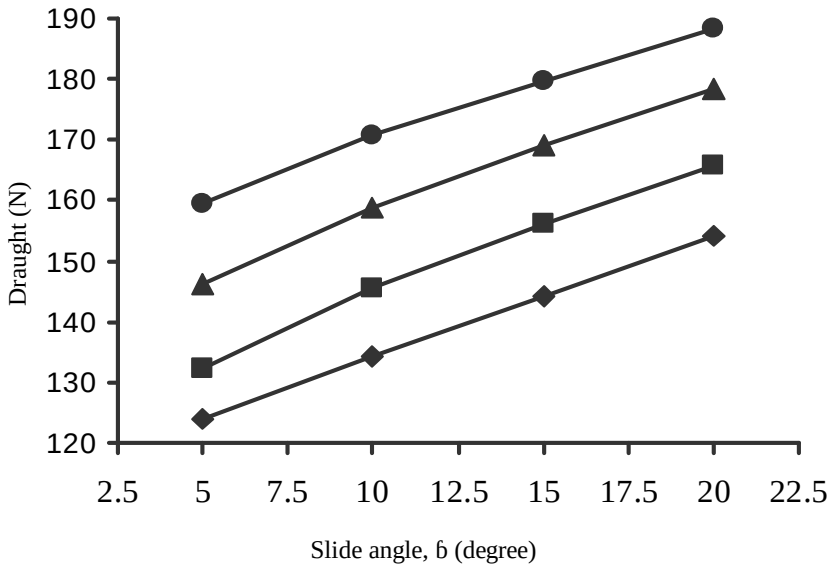


Fig. 5: Influence of slide angle and depth on draught at a speed of 15 cm/s: d=depth; d_1= 2 cm; d_2=5 cm; d_3=7.5 cm; d_4=10 cm

Figures 6-9 show the effects of nose angle, tillage depth and tool travel speed on the draught of the model tools. For each level of tool travel speed, draught increased with increases in nose angle and tillage depth. For all nose angles and tillage depths, draught increased with increases in the levels of tool travel speed. At a tillage depth of 2.5 cm and tool speed of 2 cm/s, mean draught was 76.30 N at a nose angle of 10º. For the same speed of tool movement (2 cm/s) and tillage depth of 10 cm, draught increased to 120.94 N at 10º nose angle and 145.05 N at 30º nose angle. For a tool travel speed of 15 cm/s and tillage depth of 2.5 cm, draught recorded was 124.33 N and for the same speed, draught increased to 184.23 N at a soil depth of 10 cm. These mean values of draught obtained from the interactions of depth and speed on slide and nose angles showed that draughts were significantly ($P< 0.05$) affected by both the tillage depth and tool speed.

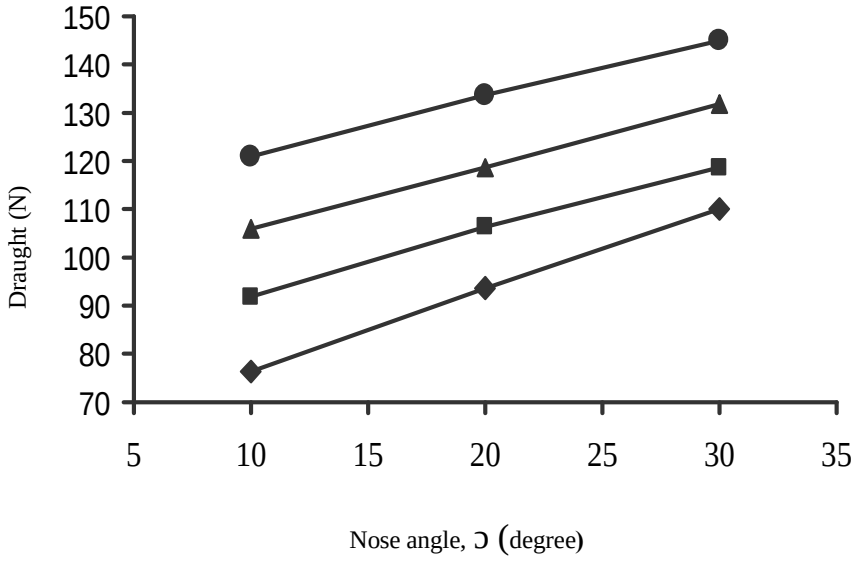


Fig. 6: Influence of nose angle and depth on draught at a speed of 2 cm/s: d=depth; D= 2 cm; d2 =5 cm; d3=7.5 cm; d4=10 cm

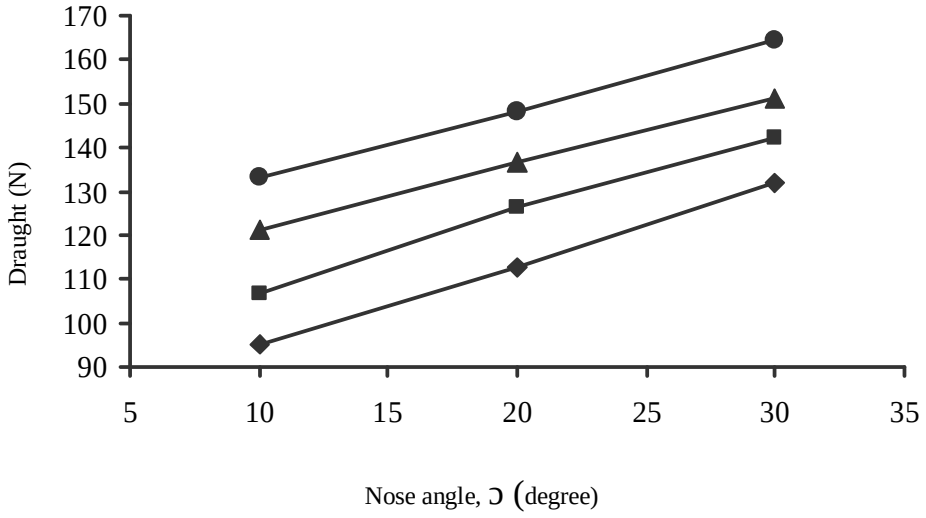


Fig. 7: Influence of nose angle and depth on draught at a speed of 5 cm/s: d=depth; D= 2 cm; d2 =5 cm; d3=7.5 cm; d4=10 cm

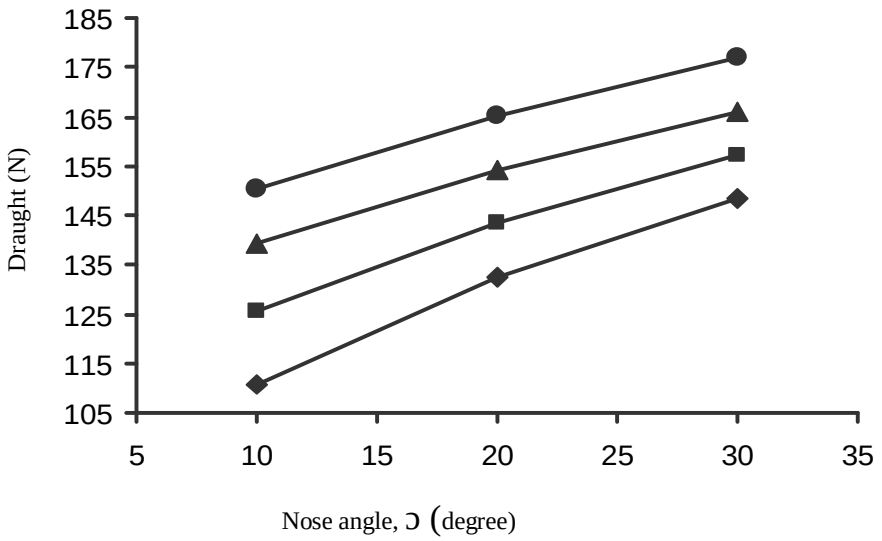


Fig. 8: Influence of nose angle and depth on draught at a speed of 10 cm/s: d=depth; D= 2 cm; d$_2$ =5 cm; d$_3$=7.5 cm; d$_4$=10 cm

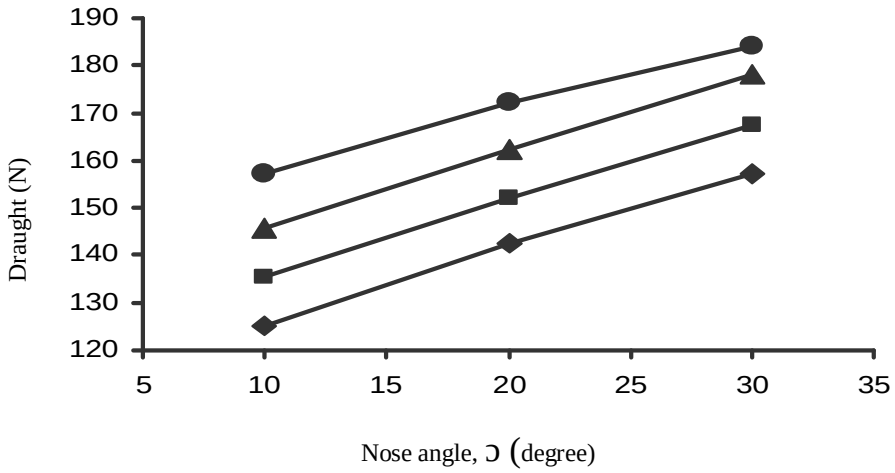


Fig. 9: Influence of nose angle and depth on draught at a speed of 15 cm/s: d=depth; D= 2 cm; d$_2$ =5 cm; d$_3$=7.5 cm; d$_4$=10 cm

Figures 10-13 present the influence of tillage depth on the interactions of slide and nose angles on draught of the model tools. For all the figures the draught increased with increases in depth, slide and nose angles. At 2.5 cm depth and 5º slide angle, mean draught was 87.63 N at 10º nose angle. For the same depth (2.5 cm) and slide angle (5º) the draught increased to 104.84 N and 114.91 N at 20º and 30º nose angles, respectively. At 2.5 cm depth and 20º slide angle, the draught increased from115.63 N at 10º nose angle to149.46 N at 30º nose angle. At the highest depth (10 cm) of tillage and 5º slide

angle, draught increased from 123.48 N at 10º nose angle to 149.93 N at 30º nose angle. For the same depth (10 cm) and 20º slide angle, draught increased from 151.39 N at 10º nose angle to 186.57 N at 30º nose angle. Figures 10 and 11 show that mean values of draught at 10º nose angles were significantly ($P < 0.05$) less than at 20º nose angles. The differences in mean values of draught between 20ºand 30º nose angles were however small. In Figures 12 and 13, the differences in mean values of draught were not significantly different among the three levels of nose angle considered.

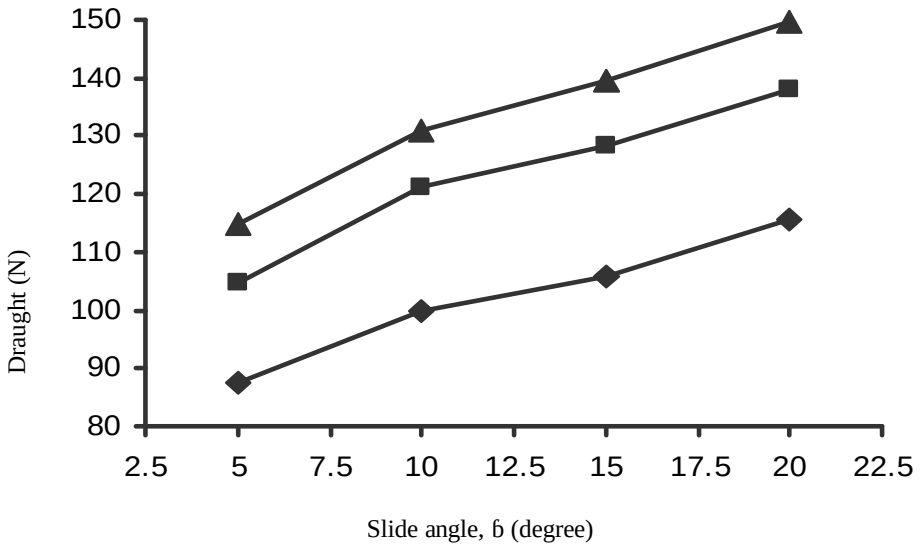


Fig. 10: Effect of the interaction of slide and nose angles on draught at a depth of 2 .5 cm: ɔ=nose angle; Dž$_1$= 10º; y ɔ$_2$ =20º; ƶ ɔ$_3$= 30º.

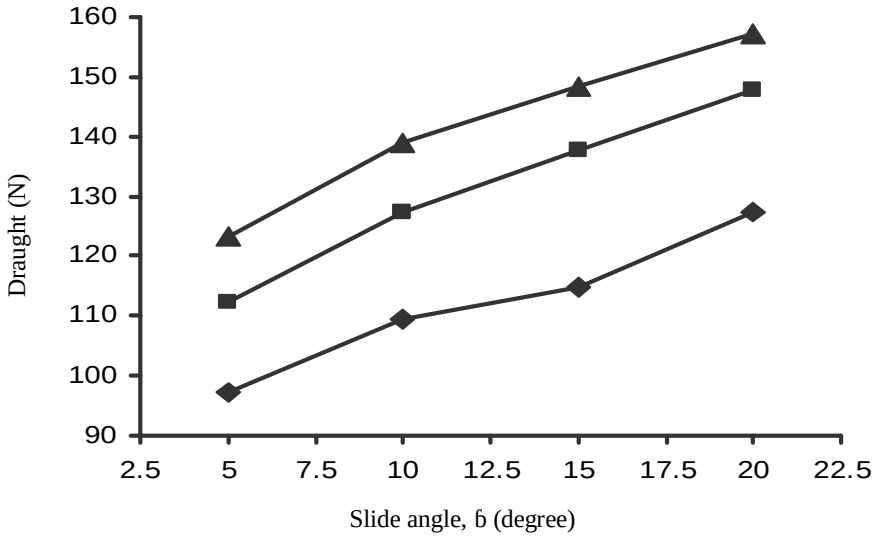


Fig.11: Effect of the interaction of slide and nose angles on draught at a depth of 5 cm: ɔ=nose angle; Dž$_1$= 10º; y ɔ$_2$ =20º; ƶ ɔ$_3$= 30º.

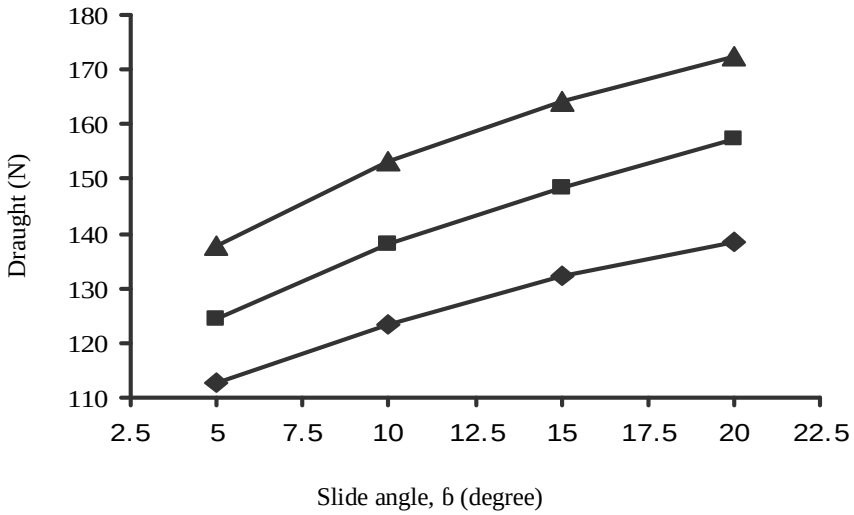


Fig. 12: Effect of the interaction of slide and nose angles on draught at a depth of 7.5 cm: ɔ=nose angle; Dž$_1$= 10º; y ɔ$_2$ =20º; ɀ ɔ$_3$= 30º.

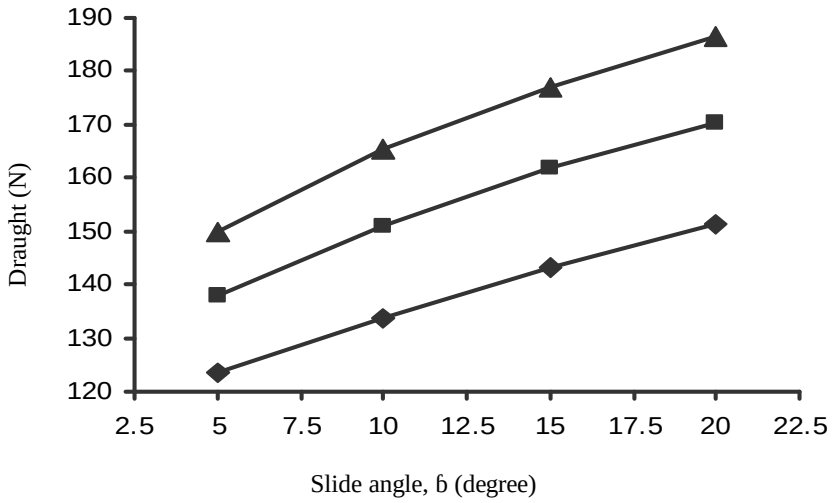


Fig.13: Effect of the interaction of slide and nose angles on draught at a depth of 10 cm: ɔ=nose angle; Dž$_1$= 10º; y ɔ$_2$ =20º; ɀ ɔ$_3$= 30º.

Figures 14-17 give the relationships of the influence of speed on the interactions of slide and nose angles on draught of the model tools. At a speed of 2 cm/s, 5º slide angle and 10º nose angle, a mean draught of 78.7 N was recorded while the same speed and slide angle gave a mean draught of 120.43 N at 30º nose angle. For the same speed (2 cm/s) and nose angle (10º), an increase in slide angle from 5º to 20º resulted in an increase in draught from 78.7 N to 116.22N, respectively. Also, at a speed of 2 cm/s and 30º nose angle, draught increased from 120.43 N at 5º slide angle to 145.94 N at

20º slide angle. When the speed was increased to 15 cm/s, a draught of 124.42 N was recorded at 5º slide and 10º nose angles. A draught of 149.25 N was obtained when nose angle was increased to 30º at same speed (15 cm/s) and slide angle (5º). At 20º slide angle and 15 cm/s tool speed, a mean draught of 155.85 N was recorded at 10º nose angle and this increased to 179.37 N at 30º nose angle. Figures 14-17 show that mean values of draught at 10º nose angles were significantly ($P< 0.05$) less than at 20º nose angles. However, the differences in mean values of draught between 20º and 30º nose angles were small.

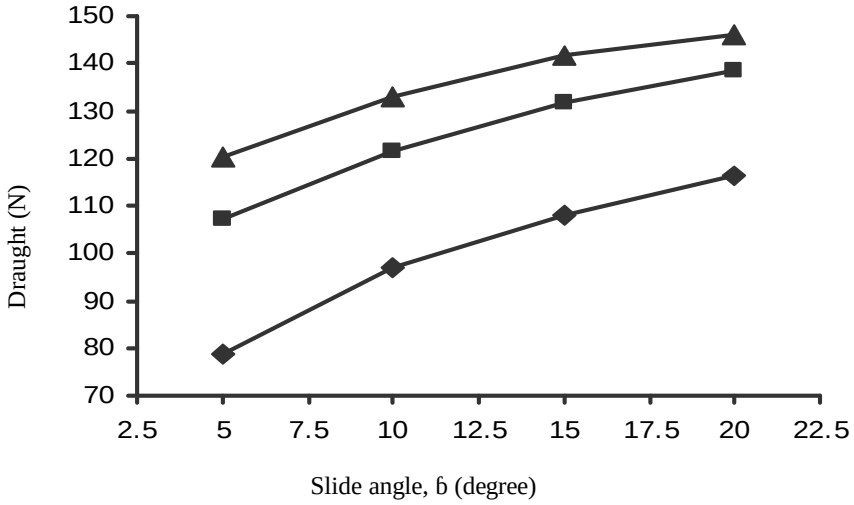


Fig.14: Effect of the interaction of slide and nose angles on draught at a speed of 2 cm/s: ɔ=nose angle; $Dž_1$= 10º; $y_{ɔ_2}$=20º; z $ɔ_3$= 30º.

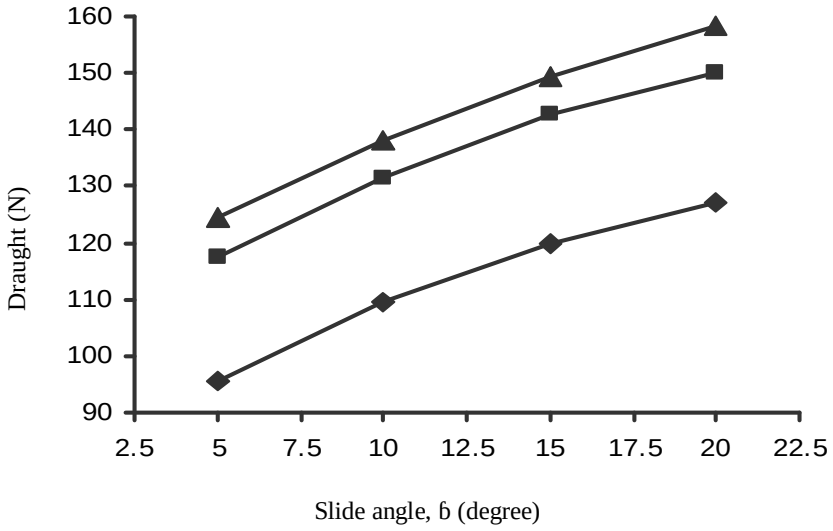


Fig.15: Effect of the interaction of slide and nose angles on draught at a speed of 5 cm/s: ɔ=nose angle; $Dž_1$= 10º; $y_{ɔ_2}$=20º; z $ɔ_3$= 30º.

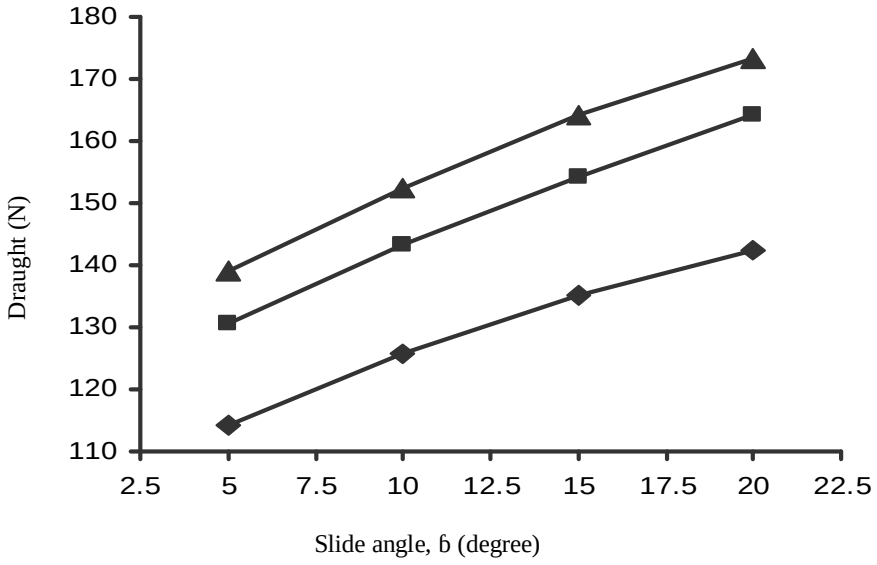


Fig.16: Effect of the interaction of slide and nose angles on draught at a speed of 10 cm/s: ɔ=nose angle; Dž$_1$= 10º; y ɔ$_2$ =20º; ɀ ɔ$_3$= 30º.

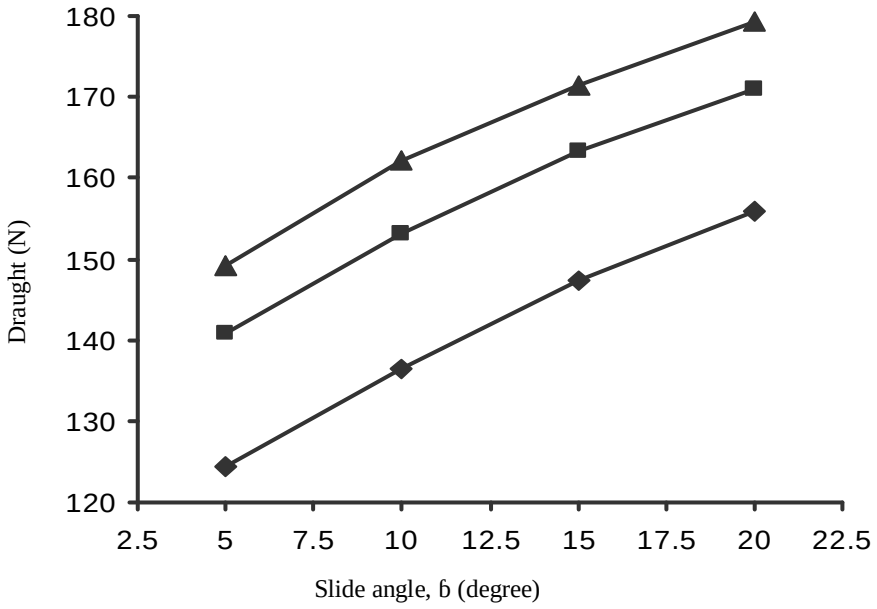


Fig.17: Effect of the interaction of slide and nose angles on draught at a speed of 15 cm/s: ɔ=nose angle; Dž$_1$= 10º; y ɔ$_2$ =20º; ɀ ɔ$_3$= 30º.

4. CONCLUSION

Model chisel furrowers were designed and fabricated for creating furrows suitable for seedling transplanting. The performances of the model tools were examined in a vertisol composed into an artificial soil in a laboratory soil bin. The artificial soil composed had properties similar to the vertisol in the field. Tool design parameters considered were slide and nose angles and operating parameters were tillage depth and tool travel speed. The effects of the interactions of depth and speed on slide and nose angles were examined. The influences of depth and speed on the interactions of slide and nose angles were also evaluated. The combined effects of the different levels of depth and speed on the various levels of slide and nose angles increased the draught of the model tools significantly. The interactions of depth and speed on slide angle gave draught values that were a little higher than those of nose angle. The effect of depth and speed on the interactions of slide and nose angles also led to increases in draught with increase in the levels of these design and operating parameters. The effect of depth on the interactions of slide and nose angles gave draught values that were slightly higher than those obtained with effect of speed. These findings show that the tool design parameters were a good combination and with proper selection of depth and speed, the tool could consume less energy in creating furrows.

REFERENCES

Al-Suhaibani, S .A. and Al-Janobi, A. 1997. Draught requirements of tillage implements operating on sandy loam soil. J. Agric. Engineering Res., 66:177-182.

Biswas, H.S., Ojha, T.P.and Ingle, G.S. 1993. Performance evaluation andoptimisation of straight blades for shallow tillage and weeding in black soils. AMA, 24(4):19-22.

Bukhari, S., Mari, G. R., Bhutto, A.B., Baloch,J.M., Mirani, A.N. and Bhutto. A. 1990. Effect of different speeds on the performance of moldboard plow. AMA, 21(1):27-31.

Fielke, J.M. 1996. Interactions of the cutting edge of tillage implements with soil. J. Agric. Engineering Res., 63: 61-72.

Gill, W.R. and Vanden-Berg, G.E. 1967. Soil dynamics in tillage and traction. Agricultural Handbook No.316. Agricultural Research Services, U.S. Department of Agriculture.

Hann, M.J. and Giessibl, J. 1998. Force measurements on driven discs. J Agric. Engineering Res., 69(2): 149-157.

Harrison, H.P. and Bai, X. 1990. Rod weeder soil reacting forces for different rod shapes and speeds. Trans. of the ASAE, 33(5): 1445-1448.

Mamman, E. 2002. Soil bin investigations of draught of model chisel furrowers in a vertisol. Ph.D. Thesis, University of Ilorin, Ilorin, Nigeria.

Manian. R., Rao, V.R. and Kathirvel, K.2000. Influence of operating and disk parameters on performance of disk tools. AMA, 31(2): 19-26, 38.

Mckyes, E. and Maswaure, J. 1997. Effect of design parameters of flat tillage tools on loosening of a clay soil. Soil Tillage Res., 43: 195-204.

Mouazen, A.M. and Nemenyi, M. 1999. Tillage tool design by the finite element method. Part 1. Finite element modelling of soil plastic behaviour. J. Agric. Engineering Res., 72: 37-51.

Natsis, A., Papadakis, G. and Pitsilis, I. 2002. Experimental investigation of the influence of the foreploughshare and the disk coulter on the tillage quality and the tractor fuel consumption. Agricultural Engineering International. Vol. IV. December, 2002.

Ohu, J.O., Arku, A.Y. and Mamman, E. 2001. Modeling the effect of organic materials incorporated into soils before load applications from tractor traffic. Ife Journal of Technology, 10 (1): 9-18.

Oni, K.C. Clark, S.J. and Johnson, W.H. 1992. The effects of design on the draught of undercutter-sweep tillage tools. Soil Tillage Res., 22:117-130.

Onwualu, A.P. and Watts R.C. 1998. Draught and vertical forces obtained from dynamic soil cutting by plane tillage tools. Soil Tillage Res., 48:239-253.

Salokhe, V.M. and Pathak, B.K. 1993. Effect of aspect ratio on soil reactions on flat tines in dry sand. J. Agric. Engineering Res., 56(3): 179-188.

Shirin, A.K.M., Hoki, M. and Salokhe, V. M. 1993. Effects of disc and working parameters on the performance of a disc plough in a clay soil. AMA, 24 (4): 9-12.

Shrestha, D.S., Singh, G. and Gebresenbet, G. 2001. Optimizing design parameters on a mouldboard plough. J. Agric. Engineering Res., 78(4): 377-389.

DEVELOPMENT AND PRELIMINARY TESTING OF METERING EQUIPMENT FOR MECHANIZED YAM SETT PLANTING

O. B. Aluko[1] and O. A. Koya[2]
[1]Department of Agricultural Engineering,
Obafemi Awolowo University, Ile-Ife, Nigeria.
[2]Department of Mechanical Engineering,
Obafemi Awolowo University, Ile-Ife, Nigeria.
E-mail address: afemikoya@yahoo.com or femikoya@oauife.edu.ng

ABSTRACT

This paper reports the design and laboratory testing of equipment for metering yam setts, as a precursory step in the development of a mechanical yam sett planter. The metering equipment was designed to discharge a yam sett at every 1000 mm of within-row spacing using a ground-wheel drive system. Yam setts flow by gravity from a hopper into a metering drum having an internal helical screw and lift flaps, which discharge the yam setts for planting. Laboratory tests of the prototype gave a metering efficiency of 82.2% with percentages of singles, multiples and skips being 80.5%, 0.2% and 17.7%, respectively. The theoretical field capacity is 0.2 to 0.4 ha h^{-1} at planting speeds of 2.7 to 5.0 km h^{-1}. The work provides a basis for the future development of a mechanical yam sett planter.

KEYWORDS: Yam sett, metering, planting, equipment, design, laboratory testing.

1.1 INTRODUCTION

Yam (*Dioscorea spp*.), a tuber crop, is a major staple food in some parts of the tropics and is also known to have a long-standing economic and socio-cultural significance in the lives of some communities (Onwueme, 1982; Hahn et. al., 1987; Degras, 1993; Otoo et. al., 2001). Yams are grown principally for the carbohydrate they provide. In Nigeria, yam constitutes over 20% of daily calorific intake (Iwueke, et al., 1983) and the country accounts for over half the total world yam production (Hahn et. al., 1987; Ihekoronye and Ngoddy, 1985). The total world production of food yam is estimated at 20 ï 25 million tonnes per year.

A large acreage of land is cultivated annually for yam production but its planting and harvesting operations are largely manual. Manual planting operation is quite inefficient and very cumbersome, requiring between 350 and 600 man-days of labour per hectare (Onwueme, 1982; Nwuba and Kaul, 1987). Traditionally, the farmers cut large tubers into setts of about 100 ï 150 g, or use small whole tubers, called seed yams, as planting materials. Seed yams, which are planted, weigh between 100 to 1500 g, are 45 ï 80 mm in diameter and 150 ï 250 mm long (Odigboh and Akubuo, 1989). Unfortunately, since seed yams are whole tubers, they are often consumed as food, resulting in a scarcity of planting material.

The shortage and the associated relatively high cost of seed yams informed the development of the minisett technique (Okoli et al., 1982). Whole yam tubers are cut into small pieces (25 g or less) called minisetts and are planted to produce seed yams. However, this technique, which is only a means to produce planting material, involves specialised cultivation activities beyond the normal scope of peasant farmers. In contrast, yam setts are culturally accepted, readily available and constitute the main planting material used by peasant farmers.

Consequently, the development of mechanical yam planters, which are compatible, in particular, with the cultural practice of yam sett planting would be worthwhile. In respect of yam sett planting, Onwueme (1982) and Odigboh and Akubuo (1989) reported that the orientation of yam setts does not affect their emergence, since any part of the sett will sprout under favourable conditions. The recommended planting depth for yam setts, reported in literature, is between 80 -100 mm below the

top of hand-made mounds or mechanized ridges, with a spacing of 1000 mm between rows and 1000 mm within rows (Irvine, 1969; Onwueme 1982). Traditionally, wider or narrower spacings may be used in ill-defined rows depending on the size of the planting material (Onwueme, 1982).

In general, very little is reported in the literature on the mechanization of yam production. Vandevenne (1973) reported on stanchion ridgers for mechanizing the planting of yams. Odigboh and Akubuo (1989, 1991) reported work on the design and development of automatic planters for planting minisetts and seed yams, respectively. However, in addition to the limitations of using seed yams and minisetts as planting materials, Aluko and Makanjuola (2002) pointed out the importance of developing a mechanical yam sett planter, which will satisfy traditional agronomic practices and will be more culturally acceptable to peasant farmers.

In separate investigations into the mechanization of yam planting, different researchers have reported satisfactory results using planting units that are similar in design (Aluko, 1983; Odigboh and Akubuo, 1991; Aluko and Makanjuola, 2002). In contrast, choking and/or blockage at the hopper throat on account of the size, shape and frictional characteristics of yam planting materials, particularly yam setts, have plagued earlier efforts to develop metering systems for mechanized yam planting (Akubuo et al., 1987; Akinlade and Solaja, 1997; Tomori, 2002).

Indeed, it has been pointed out (Odigboh and Akubuo, 1991) that, in the development of a yam planter, the metering mechanism represents the major work of innovation. This report describes the design of new equipment for metering yam setts from the hopper into the delivery manifold of a mechanical yam sett planter.

The objectives of this work were: to design and fabricate equipment for metering yam setts, test the metering equipment in order to evaluate its performance and predict machine theoretical field capacity.

2. MATERIALS AND METHODS

2.1 Design Principles and Considerations

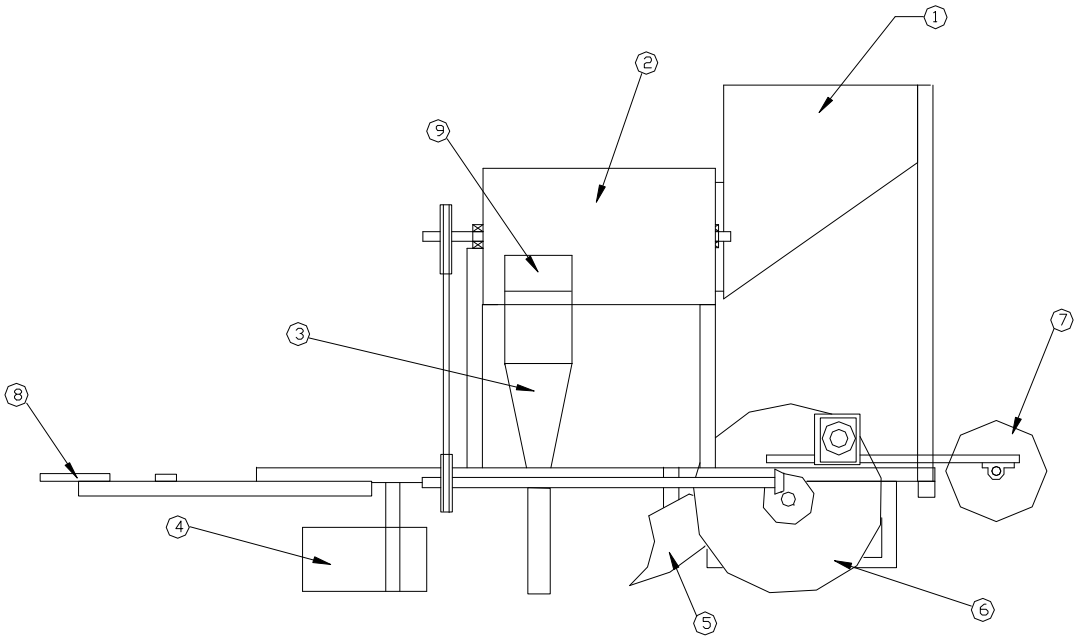
The metering equipment was conceived as a simple device for transferring yam setts from a hopper into the delivery tube of a tractor-mounted yam planter, without bruising the *periderm* of the setts. Also, the equipment should be easy to fabricate and usable by anybody, even without any previous technical training.

The metering equipment was designed using basic engineering principles. Details of materials specifications, selection and design calculations for the machine components are presented in Appendix A.

Table 1 shows the dimensions of the major components of the equipment. The envisaged planter, equipped with the metering equipment, will be hitched to a tractor as shown in Fig. 1. The metering mechanism is ground-wheel driven so that, the within-row spacing is independent of the tractor forward speed.

Table 1. Specification of major components of the metering equipment

Hopper		
Upper aperture (trapezoidal)		
parallel sides,	mm	450, 280
height,	mm	500
Base Panel (rectangular),	mm	610 x 280
Inclination of base panel,	deg.	35
Metering Drum		
Outer drum		
diameter,	mm	350
length,	mm	600
Inner drum		
diameter,	mm	280
length,	mm	450
Worm (laid on inside of inner drum)		
pitch,	mm	100
height	mm	100
Flap	mm	90 x 30



2.2 Description of the Yam Sett Metering Equipment

The orthographic views of the equipment are shown in Fig. 2. The hopper, made from gauge 16 mild-steel sheet, has trapezoidal cross-section and its base was inclined at 35^o to the horizontal to discharge by gravity into the metering drum. Its exit is a circular chute with a semi-circular lip to guide the setts into the metering drum. The hopper was designed to hold 200 pieces of yam setts with average diameter of 80 mm and so, containing enough planting materials for 0.2 ha of farmland at a time. The hopper was bolted to the supporting frame and can be easily detached for cleaning when necessary.

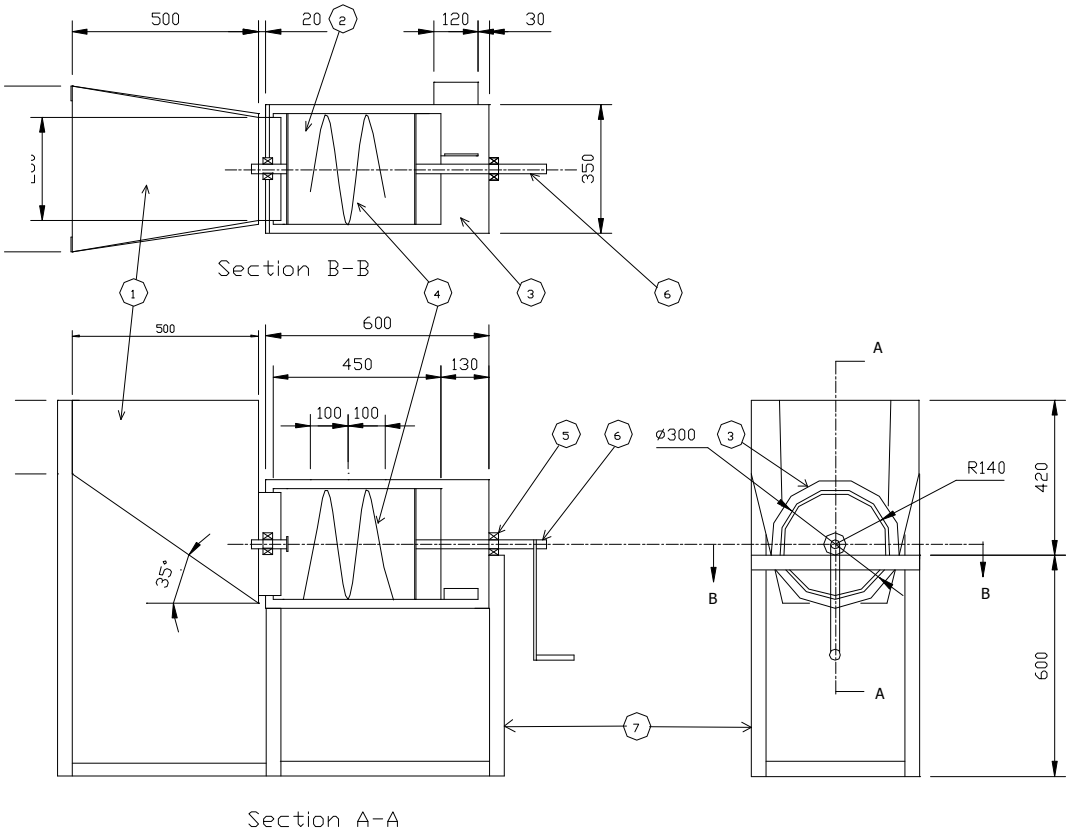


Fig. 2 Orthographic views of the yam sett metering equipment: 1, Hopper; 2, Inner metering drum; 3, Outer drum; 4, Worm; 5, Bearing; 6, Shaft; 7, Frame

The metering drum consists of two co-axial cylinders, an outer drum (ϕ350 x 600 mm long) and an inner drum (ϕ280 x 450 mm long). The outer drum was welded to the supporting frame whereas the inner drum was welded to a 25 mm shaft, which was supported on two bearings, one on a support across the exit of the hopper and the other on the supporting frame. The inner drum was equipped with internal helical screw (100 mm pitch and 100 mm high) running through its length. The shortfall in the length of inner drum compared with the outer drum provided for clearance against the hopper's lip at one end, and the other end provided room for a metal flap, attached to the inner drum. The flap sweeps metered setts, picking one sett at a time until it drops out, through a slot in the outer drum, into the delivery manifold of the planter.

The frame was constructed from 40 x 40 x 4 mm angle iron. Its overall dimension was about 1100 mm long, 450 mm wide and 820 mm high. A handle was fixed on the shaft, to drive the equipment during laboratory tests. A photograph of the prototype showing its two major parts, namely the hopper and the metering drum, is presented in Fig. 3.

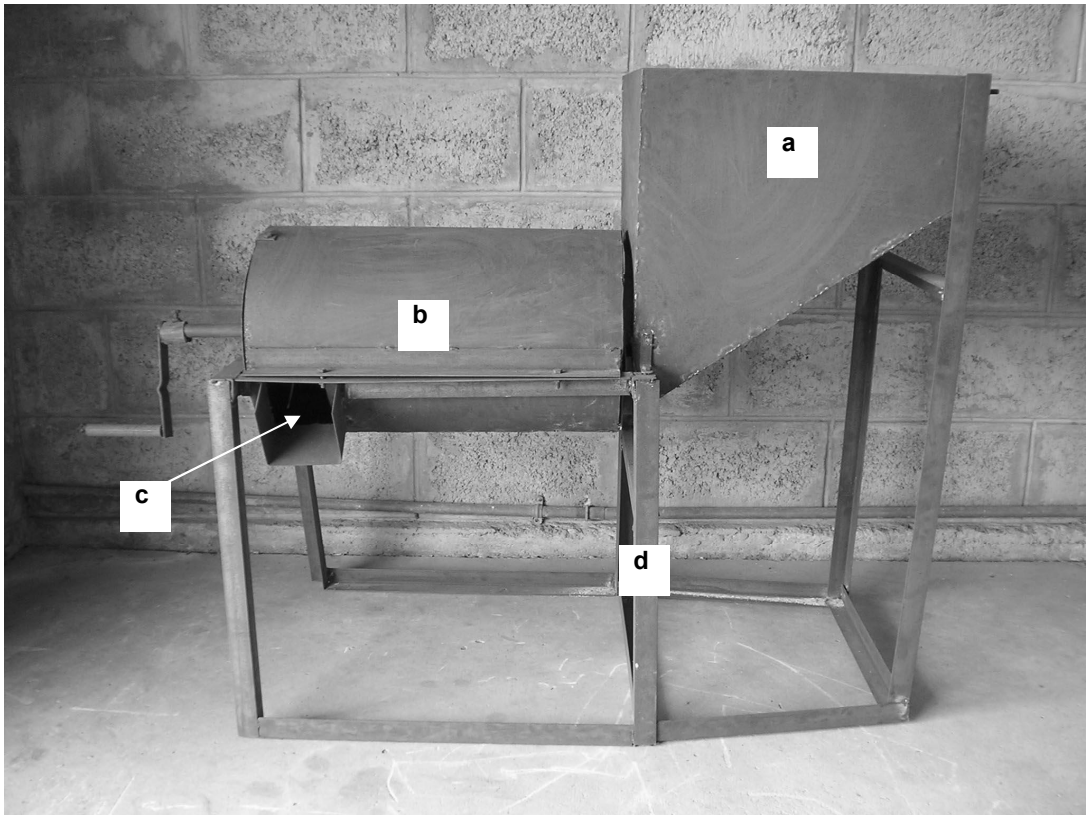


Fig. 3. Photograph of the yam sett metering equipment: a, hopper; b, metering drum; c, sett ejection slot; d, frame

2.3 Experimental Procedure for Laboratory Testing

Yam tubers were obtained from local farmers in Ile-Ife, Nigeria, and were cut into setts with average diameter of about 80 mm. The setts were then stored in a dry, well-aerated environment for two days, as is the practice in traditional yam planting (Onwuneme, 1982). This also helped in reducing the possibility of the setts adhering to the panels of the hopper (Ajav, 1998; Aluko and Koya, in press).

The hopper was filled with yam setts and the metering drum was driven at approximately 45 rev/min. For each experimental run, which consisted of eight revolutions of the metering drum, the number of setts discharged was noted. The actual number of setts delivered was counted and compared with the number expected based on design.

Equipment performance was then quantified in terms of its metering efficiency (ε_m) and the corresponding percentages of skips, singles and multiples (Kepner et. al., 1987). The metering efficiency is an indication of how many stands on the field, will actually receive setts for planting, and was defined as,

$$\varepsilon_m = \frac{N_d}{N_T} x100\% \qquad \text{--- --- (1)}$$

where, N_d is the number of times setts (single or multiple) were delivered; and N_T is the number of times sett delivery was expected, for the same rotations.

Metering efficiency was considered to be a better performance index than the percentage cell-fill, often specified for grain drills (Kepner et. al., 1987). In percentage cell-fill, empty cells are offset by extra seeds in multiple fills and, not necessarily that every cell contains a single seed. Percentage of skips is the ratio of times with no sett delivered to the number of times sett delivery was expected. Percentages of singles and multiples are the number of times single sett and multiple sett delivery, respectively, were observed, compared with the number of times setts should be delivered. Furthermore, the discharged setts were examined physically to see if the *periderm* was bruised.

The theoretical field capacity of the prototype was estimated, for a two-row planter equipped with the metering equipment at recommended speeds of 2.7 to 5.0 km h^{-1} (Odigboh and Akubuo, 1989; Aluko and Makanjuola, 2002). The estimate was adjusted incorporating the metering efficiency as follows:

$$C = \frac{sw}{10} x \varepsilon_m \quad \text{--- ---} \quad (2)$$

where, C is the theoretical capacity in ha h^{-1}; S is the speed of travel in km h^{-1}; and W is the width of implement in m.

3. RESULTS AND DISCUSSION

The results of the tests carried out to evaluate the performance of the metering equipment are shown in Table 2. The prototype metering equipment has a hopper holding capacity of 37.5 kg. A metering efficiency of 82.2% was obtained and the percentages of singles, multiples and skips were 80.5%, 0.2% and 17.7%, respectively. As pointed out earlier, the size, shape and frictional characteristics of yam planting materials pose major challenges in the development of metering equipment. Odigboh and Akubuo (1991) reported a metering efficiency of about 98% for a minisett yam planter. Compared to yam setts (100 ï 150 g) and seed yams (100 ï 1500 g), however, minisetts (about 25 g or less) constitute much smaller planting material. The metering efficiency of the seed yam planter earlier developed by Odigboh and Akubuo (1989) was not specified, thus precluding a comparison with the present results.

Table 2. Performance of the prototype metering equipment

Performance indices		Value ± standard error
Hopper, capacity,	kg	37.5
Metering efficiency,	%	82.2 ± 4.5
Percentage of singles,	%	80.5 ± 4.1
Percentage of multiples,	%	0.2 ± 0.8
Percentage of skips,	%	17.7 ± 4.1

The percentage of multiples though low, implies that in some instances, two, rather than one sett, were dropped but planting (sett delivery) actually took place. For subsequent field tests of the envisaged planter, this anomaly can be alleviated by incorporating a stationary brush to knock out the excess planting material when the flap lifts more than one sett. During the tests, the sharp leading edge of the worm occasionally scratched a few of the setts. It is therefore necessary to shield the sharp leading edge of the worm with a softer material like rubber to reduce the occurrence of bruising the setts.

The percentage of skips obtained in the present results (17.7%) needs to be reduced/eliminated to justify the use of a mechanical planter to replace traditional manual planting. The present results suggest that there is a need to increase the pitch of the worm and the clearance between the inner and the outer drums, to facilitate the worm picking setts without any failure. The required adjustments indicate that yam setts for planting would need to be sorted into size groups prior to loading them into

the hopper. This modification will also enhance a satisfactory performance of the metering equipment at different tractor field speeds.

For a within-row spacing of 1000 mm and a planting speed range of 2.7 to 5.0 km h^{-1}, the estimated field capacity ranged from 0.2 to 0.4 ha h^{-1}.

4. CONCLUSION

Equipment for metering traditional yam setts for mechanical planting has been developed. The preliminary tests carried out in the laboratory on the prototype indicate a fairly satisfactory performance. It should be possible to improve the performance of the equipment for field applications, especially with respect to hopper capacity and reducing the percentage of skips, with further modifications and testing.

REFERENCES

Ajav, E. A., 1998. Engineering properties of yam setts as related to mechanization of yam planting. Journal of Root Crops, Vol. 24 (2): 171 ï 176.

Akinlade, O. and Solaja, O., 1997. The design and construction of a low cost mechanical yam planter. B.Sc. Thesis, Department of Agricultural Engineering, Obafemi Awolowo University, Ile-Ife.

Akubuo, C.O., Odigboh, E.U. and Anazodo, U.G.N., 1987. Design of a two-row automatic seed yam planter. Paper presented at the 2nd International symposium on the yam tuber. Anambra University of Technology, Enugu, Nigeria.

Aluko, O.B., 1983. Studies of the mechanisation of yam planting with particular reference to models of planting devices. B.Sc. Thesis, Department of Agricultural Engineering, University of Ife (now Obafemi Awolowo University, Ile-Ife), Nigeria.

Aluko, O.B. and Koya, O.A., in press. Some engineering properties of yam setts from two species of yams. Journal of Food Engineering, Elsevier Science Ltd.

Aluko, O.B. and Makanjuola, G.A., 2002. Preliminary studies of some agronomic and design factors relevant to the mechanization of yam sett planting on ridges. Journal of Agricultural Engineering and Technology. Vol. 10: 17 ï 27.

Degras, L., 1993. The yam. a tropical root crop. The Macmillan Press Ltd., London pp. 408.

Hahn, S. K., Osiru, D. S. O., Akoroda, M. O., anad Otoo, J. A., 1987. Yam production and its future prospects. Outlook on Agriculture, Vol. 16 (3): 105 ï 110. Pergamon Journals Ltd., Great Britain.

Hamrock, B. J., Jacobson, B. O., Schmid, S. R., 1999. Fundamentals of machine elements. The McGraw ï Hill Companies, Boston, USA. Pp 423 ï 432.

Ihekoronye, A. I and Ngoddy, P. O., 1985. Integrated food science technology for the tropics. Ist edition. Macmillan Publishers, Ltd., London. pp. 127 ï 220.

Irvine, F. R., 1969. West african crops. Vivian Ridler Oxford University Press, London. 3rd edition pp. 153 ï 188.

Iwueke, C. C., Mbata, E. N., and Okereke, H. E., 1983. Rapid multiplication of seed yam by minisett technique. National Root Crop Research Institute, Umudike, Nigeria. Research Bulletin No. 9.

Kepner, R. A., Bainer, R., and Barger, E. L., 1987. Principles of farm machinery. First Indian, Edition. CBS Publishers and Distributors, India. Pp. 209 ï 230.

Nwuba, E. I. U and Kaul, R. N., 1987. Human energy requirement of typical Nigerian traditional tillage tools. African Journal of Science and Technology, Series A Vol. 6 (1): 20 ï 28.

Odigboh, E. U. and Akubuo, C. O., 1989. A two-row automatic seed yam planter prototype. Proceedings of the Eleventh International Congress on Agricultural Engineering. Dublin, Ireland 4 ï 8th September, 1989 pp. 1703 ï 1709.

Odigboh, E. U. and Akubuo, C. O., 1991. A two-row automatic minisett yam planter. Journal of Agricultural Engineering Research 50: 189 ï 196.

Okoli, O.O., Igbokwe, M. C., Ene, L. S. O and Nwokoye, J. U., 1982. Rapid multiplication of yam by minisett technique. National Root Crops Research Institute, Umudike, Nigeria. Research Bulletin No. 2.

Onwueme, I.C., 1982. The tropical tuber crops: yams, cassava, sweet potato and cocoyams. John Wiley and Sons. London, Chichester.

Otoo, J. A. Okoli, O. O. and Ilona P., 2001. Improved production of seed yam. International Institute of Tropical Agricultural (IITA) Research Guide 63. IITA, Ibadan, Nigeria.

Tomori, O.O., 2002. The development of a hopper and metering system for planting yam setts. B.Sc. Thesis, Department of Agricultural Engineering, Obafemi Awolowo University, Ile-Ife.

Vandevenne, R., 1973. Mechanization of yam cultivation in the Ivory Coast. Proceedings of the Third Symposium of the International Society for Tropical Root Crops. IITA. Ibadan, Nigeria.

NOTATION

ε_m	-	metering efficiency
N_d	-	number of times setts (single or multiple) were delivered
N_T	-	number of times setts delivery were expected based on design
C	-	theoretical field capacity, ha h^{-1}
S	-	speed of travel, km h^{-1}
W	-	width of implement or, between row spacing for a two-row planter, m

APPENDIX A
Design of Major Components of the Yam Set Metering Equipment

A. 1 The hopper

The hopper was made from guage 16 mild steel sheet, formed and welded to hold 200 pieces of yam setts, 80 mm average diameter. The following limiting values of properties of fresh yam setts, reported by Aluko and Koya (in press) were used:

Yam bulk density, $\rho = 1120$ kg m^{-3}
Maximum coefficient of friction, $\mu = 0.5$

Hence, for free flow, the following relationship between the angle of inclination θ and the coefficient of friction prevails:

$$\tan\theta \geq \mu \qquad \text{---} \qquad \text{---} \qquad (A.1)$$

Therefore, $\theta \geq \tan^{-1}(0.5)$ or 27^o

The design angle was chosen to be 35^o, about twenty - percent above the calculated value.

A. 2 The Internal Helical Screw

The internal helical screw (worm), welded inside the inner drum, was made from gauge 18 mild steel sheet. This thickness was selected to make fabrication easy. The diameter *D* to form a helix of certain diameter d and pitch length *p* can be determined from:
a

$$(\pi D)^2 = (\pi d)^2 + p^2 \qquad \text{---} \quad \text{---} \quad \text{---} \qquad (A.2)$$

This expression was used to calculate the internal and external diameters of circular plates used in forming the helices.

A. 3 The Power Transmission Elements

The basic transmission elements in the design are the shaft and the supporting bearings, and the turning handle. The shaft was designed based on the following assumptions: shaft is solid, and made from low-carbon steel (AISI 1020); shaft length, from bearing to bearing, is 650 mm; density of shaft material is 7860 kg m^{-3}; yield strength of shaft material is 295 MPa; factor of safety, n_s is 2.5.

Shaft was designed on account of rigidity and strength, based on distortion energy theory (DET), which predicts the smallest diameter where failure will first start to occur. According to Hamrock et al. (1999),

$$d = \left[\frac{32 n_s}{\pi s_y} \sqrt{M^2 + \frac{3}{4} T^2} \right]^{1/3} \qquad (A.3)$$

Based on calculations and available material, a conservative 25.4-mm diameter shaft was chosen. Appropriate SKF deep groove ball bearings (6005) suitable for the shaft were selected.

The handle was made from a 20 x 3 mm flat bar, L ï shaped, with a hollow pipe at the free end to engage the shaft, the other bent end provided handle for turning.

AN EXPERIMENTAL MECHANICAL CASSAVA TUBER PEELING MACHINE

D. A. Adetan[1], L. O. Adekoya[1], O. B. Aluko[2] and G. A. Makanjuola[2]
[1]Department of Mechanical Engineering, Obafemi Awolowo University, Ile-Ife, Nigeria
E-mail: aadetan@yahoo.com; dadetan@oauife.edu.ng;
[2]Department of Agricultural Engineering, Obafemi Awolowo University, Ile-Ife, Nigeria

ABSTRACT

Previous cassava peeling research efforts were directed mainly towards developing abrasive type batch peelers. In peeling with most of these peelers, however, big roots remain largely unpeeled while small ones may be completely grated. In this work, an experimental mechanical cassava peeling machine that works on the principle of peel-flesh separation by compression and peel removal with knives was designed and fabricated. It comprised of a horizontal belt conveyor unit and a spring-loaded knivesô unit. In operation, the belt conveyor unit conveys slices of cassava tubers which are peeled under an array of spring-loaded knives. Preliminary tests of the machine were carried out on root slices of different sizes with the conveyor belt driven at a linear speed of 1.31 m/s. For root slices having mid-section diameters ranging between 45 and 55 mm, the peel removal efficiency ranged between 0.920 and 0.973 and had an average value of 0.939. For slices having mid-section diameters ranging between 55 and 65 mm, the peel removal efficiency ranged between 0.953 and 1.000 and had an average value of 0.988. For tubers in the above size ranges, no breakage of roots occurred during peeling. For root slices with relatively larger diameters, however, the peel removal efficiency ranged between 0.152 and 0.820 and root breakage was observed to occur in some instances. In all cases, however, there was no loss of useful tuber flesh.

KEYWORDS: Design; cassava root tuber; peeling machine; preliminary tests; peeling efficiency

1. INTRODUCTION

Cassava (*Manihot esculenta* Crantz) is one of the most common economic and productive root crop in the tropics. Its root tuber is the main economically useful part of the plant. Cassava possesses vast food and industrial potentials. It is arguably the largest single crop of the tropics, particularly of that part of Africa lying south of the Sahara and north of the Zambezi, where it has become the most important crop in terms of both the total land area devoted to its production and the proportion it contributes to the human diet (Odigboh, 1983).

Before the cassava tuber is processed into any of its food and some of its non-food products, however, it must be peeled. Peeling is simply the removal of the cassava peel (made up of the outer corky periderm and cortex) from the rest of the tuber. Ideally and especially in the food industry, the peel needs to be completely removed without removing the useful tuber flesh.

The problem encountered in peeling cassava root tubers arises from the fact that cassava roots exhibit appreciable differences in weight, size, shape, peel thickness, peel texture and strength of adhesion of peel to the root flesh. Furthermore, these properties vary with the month of the year during which the root is harvested and the time that elapses after harvesting, before peeling is done. The ease of peeling varies with these properties. The greatest challenge in the design of a cassava peeler is that of making the machine capable of efficiently peeling roots from all sources all the year round despite the wide differences in these properties. As a result, the development of a technically or economically acceptable cassava tuber peeling machine has continued to pose a challenging engineering problem. Existing machines tend to reduce the cassava tuber to a regular cylinder, thus wasting an intolerably high proportion of the useful cassava flesh before all the peel is removed.

Researchers have experimented with various types of abrasive drums for batch peeling of cassava roots. Suleman (1980) described the vertical drum type; Akinrele et al (1971) described the concrete mixer shape type; Ezekwe (1979) and Nwokedi (1984) in separate investigations reported the

development of horizontally-mounted drum peelers that are similar in principle; Odigboh (1988) reported the eccentrically mounted drum type. Though these machines are simple to fabricate and operate, it is generally difficult for the abrasive surfaces of the drums to enter into the crevices and depressions on tuber surfaces. A tuber may be reduced to a cylinder of uniform radius with much wastage of useful flesh before satisfactory peeling is done. Otherwise, hand trimming is required to finish incompletely peeled roots. Although Ezekwe (1979) and Odigboh (1988) reported some improvement by using a technique in which abrasive balls are mixed up with the cassava roots before being loaded into the drums, the balls easily become blunt and ineffective after a few peeling batches.

Odigboh (1976) reported a cylindrical knife cassava root peeler, which basically consists of a cylindrical knife assembly mounted parallel to a solid cylinder with roughened surface. Both were driven clockwise at different speeds. The cassava roots to be peeled were cut into 10cm lengths and fed into the space between the knife assembly and the solid cylinder. Although a peel removal efficiency of 75% and average throughput of 165 kg/h were reported, hand trimming was still required to complete the peeling.

Ohwovoriole et al. (1988) reported a simple test rig for peeling cassava tuber slices manually (Figs. 1(a) and (b)). The rig consists of evenly spaced cutting edges mounted on two

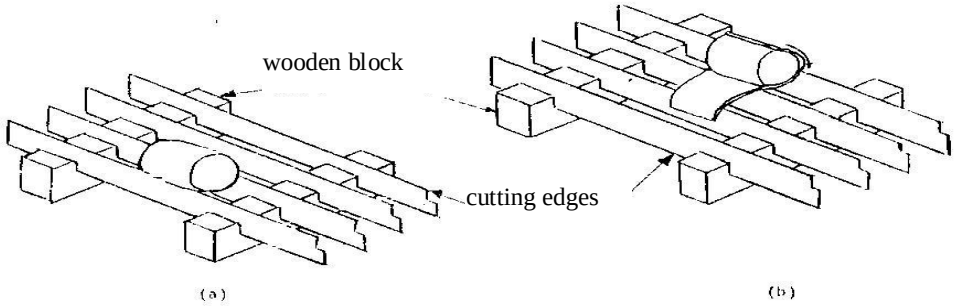


Fig. 1. Test rig for peeling cassava tuber slices manually (after Ohwovoriole et al., 1988).

wooden blocks. The cassava tuber slice resting on it is peeled manually by pushing down on it with the hand; the cutting edges penetrate through the peel into the cambium and, as the slice is rolled forward while the downward pressure is maintained, the peel simply unwinds from the flesh as shown in Fig. 1(b). Based on the principle illustrated by this rig, Ohwovoriole et al. (1988) developed a manual cassava tuber peel lacerating machine. The machine consists essentially of a fixed outer frustum of a cone, which was made up of rigid longitudinal cutting edges, and a rotating wooden inner cylinder. Although a peel removal efficiency of 92% was reported after a limited test run, the machine did not provide for the automatic adjustment of the size of the space between the inner cylinder and the outer cutting edges, which is required to accommodate varying sizes of root slices. A root slice would therefore be crushed, rather than peeled, if it gets into a space where the distance of separation between the outer cutting edges and the wooden inner cylinder is much less than the diameter of the root slice. The principle employed is however quite promising for there was reportedly no loss of useful tuber flesh during peeling.

The objective of this work was to design and construct an experimental cassava root tuber peeling rig on which experiments could be run to determine the optimum design and operating characteristics of a machine that would be developed using the principle reported by Ohwovoriole et al. (1988).

2. MATERIALS AND METHODS

2.1 Design Principles and Considerations

The concept used to develop the present mechanical peeler is illustrated in Fig. 2 and is based on the peeling principle employed by the manual test rig shown in Figs. 1(a) and (b). In Fig. 2, the human hand is replaced by a pressure application platform for applying pressure to, and rolling the tuber over an array of cutting knife edges. The questions that arise in the attempt to employ this peeling concept and which the experimental peeler described in this work has been designed to address are:

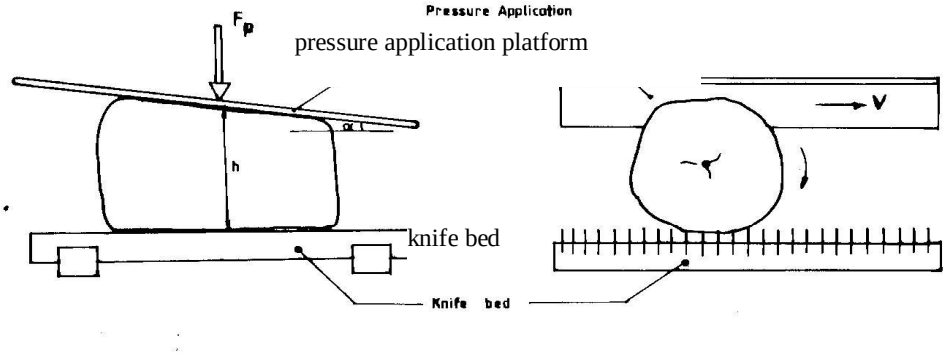


Figure 3.3: Root slice rolling between a moving pressure application

Fig. 2. Root slice rolling between a moving pressure application platform and a bed of knives.

(i) what must be the average distance between the pressure application platform and the cutting edges for a given diameter of roots such that good peeling would be effected?
(ii) at what speed must the pressure application platform move relative to the cutting edges as it rolls the tuber along without slippage?
(iii) what magnitude of the force needs to be applied to the root slice to effect peeling and yet avoid crushing the slice?

2.2 Description of the Experimental Peeling Machine

A photograph of the experimental peeling machine is shown in Fig. 3. Three orthographic views of the machine are also shown in Fig. 4. The machine comprised two units: an upper spring-loaded knivesôunit and a lower horizontal belt conveyor unit.

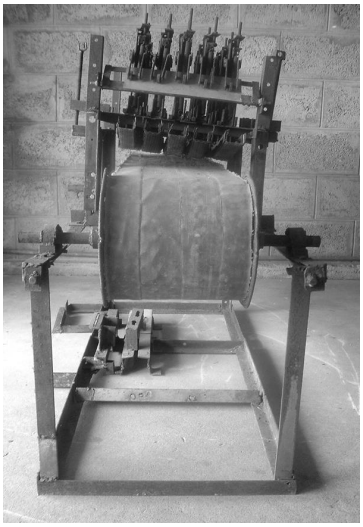


Fig. 3: The experimental peeling machine

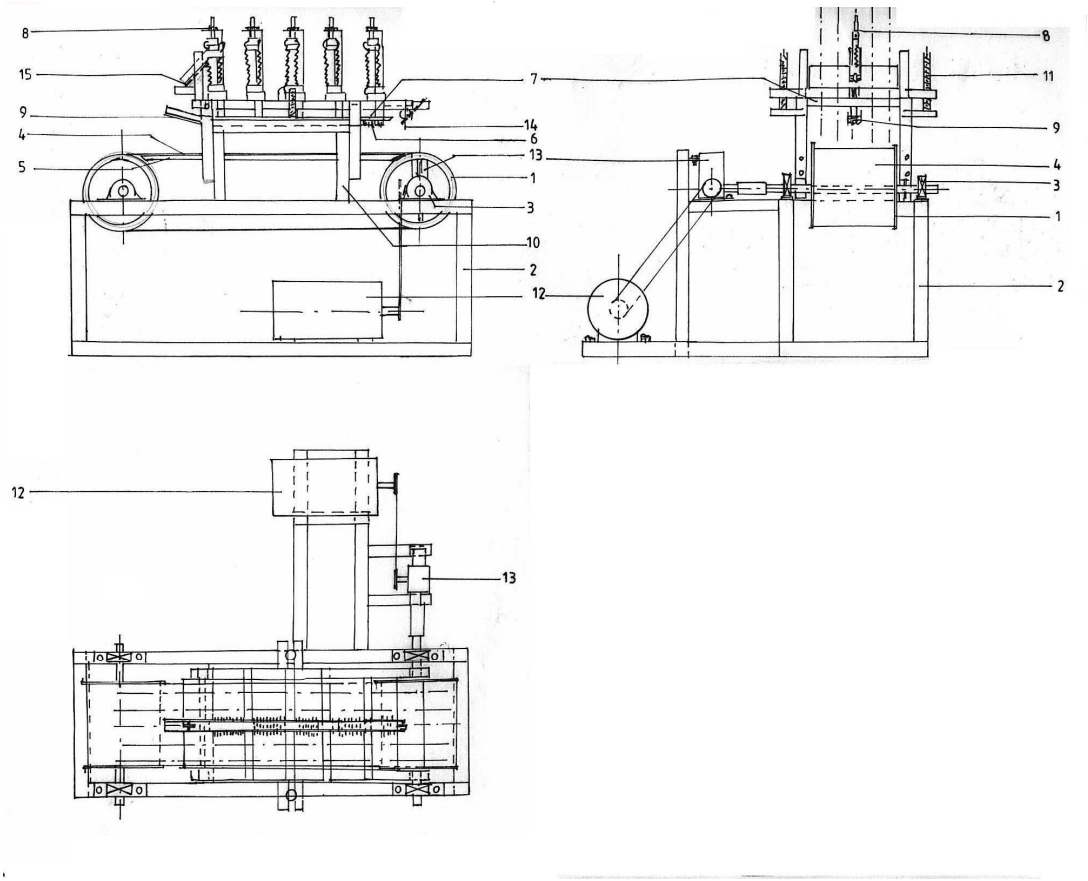


Fig. 4. Orthographic views of the experimental cassava peeling machine in first angle: 1, Conveyor drum; 2, Main frame; 3, Bearing; 4, Conveyor belt; 5, Conveyor belt platform; 6, Peeling blades; 7, Knife assembly bearing frame; 8, Spring load adjuster nut; 9, Root pick-up; 10, Main frame link arm; 11, Knife bed height adjustment screw; 12, Variable speed electric motor; 13, Speed reduction gear box; 14, Rear roller motion guide plane; 15, Front roller motion guide plane.

In the belt conveyor unit, the drums (1) are mounted on a rectangular main frame of angle iron (2) via bearings (3). The centres of the drums are spaced 1050 mm apart and each of the drums measures 250 mm in diameter and 300 mm in length. The belt (4) of the conveyor system is 300 mm wide. This belt was designed to move over a flat aluminum sheet platform (5) lying on top of a frame of angle iron. The platform was rigidly fixed to the frame of angle iron using bolts and nuts. The belt conveyor was driven by a 1.5 kW variable speed electric motor (12) through a speed reduction gear box (13) and a chain drive.

The knife assembly bearing frame of the upper spring-loaded knivesô unit is 800 mm long and 400 mm wide. The unit comprises of five assemblies of peel penetrating knives, arranged across the central 290 mm of the 400 mm width of the rectangular frame. Each assembly is 600 mm long and 50mm wide. The knife assemblies are spaced 10mm apart across their bearing frame. A root pick-up (9) inclined at 15^0 to the surface of the conveyor belt is fixed to the frontal end of each knife assembly. It is wrapped around with a sheet of expanded metal to enhance its grip on the root.

Five spring-loading points, equally spaced at 140 mm intervals, were located along the length of each knife assembly. A set of two 140 mm long helical tension springs, each of which has a spring rate of 2.193 N/mm, was located at each spring-loading point. Thus, there were a total of 25 such pairs of springs in the spring-loaded knives unit. This design of the spring-loading system was based on an earlier work by Adetan et al. (2003) in which the peel penetration force per unit length of knife edge

was determined. The tensile load in these springs can be adjusted by turning the spring load adjuster nuts (8). It is this tensile load in the springs that determines the downward force on the knife assembly and, therefore, the force with which the knives attempt to penetrate into the peel of the cassava roots being conveyed under them. Each knife assembly carries 120 knives that are spaced 5 mm apart. Each knife is about 1.5 mm thick, 50 mm long and 15 mm wide. It is made from galvanized iron sheet and one of its 50mm edges is sharpened to form the lower peel penetrating edge.

It is expected that a knife assembly will not only move vertically in response to the root size but it will also tend to move horizontally in the direction of motion of the belt in response to the rolling resistance force in play between the knives and the root. Thus, front and rear rollers are provided on the knife assembly to enhance a frictionless motion. The rollers roll on roller motion guide planes (14 and 15) inclined at 45° to the horizontal and bolted to the knife assembly bearing frame. By this arrangement, the motion of the knife assembly is constrained and made frictionless.

Using bolts and nuts, the knife assembly bearing frame (7) is connected to the main frame link arms (10) (Figs. 4) through the slots in the four legs of the frame. The height of the knife bed above the conveyor belt can be adjusted by loosening these bolts and nuts, turning the square-threaded height adjustment screws (11) on either side of the knife assembly bearing frame until the desired height is reached and then tightening the bolts and nuts again. In this same manner, the lateral angle of inclination of the knives to the conveyor belt surface (across the belt width) can also be adjusted to suit the taper of the root surface from its proximal to its distal end.

2.3 Experimental Procedure for Testing

The root tubers used to test-run the experimental peeler were obtained from cassava plants aged between 18 and 20 months. Fresh roots randomly chosen from two IITA cultivars (TMS 30572 and TMS 30555) of the bitter cassava type commonly grown in Ile ï Ife, Nigeria, were used. The roots were run in the machine within 12 hours of harvesting. They were prepared for the tests by cutting them into 100mm long near cylindrical tubers. The diameters of a tuber at its proximal end, middle section and its distal end were measured using a pair of vernier calipers and recorded as d_1, d_2, and d_3 respectively. The average of d_1, d_2, and d_3 was subsequently computed and denoted d. The roots were then sorted into middle section diameter size groups of 45ï 55 mm, 55ï 65 mm, 65ï 75 mm, 75ï 85 mm and 85ï 95 mm. The angle of inclination of the knife bed to the surface of the conveyor belt across its width, α, was set at about 5.3°. This is the average degree of taper of the typical root surface from its proximal to its distal end (Adetan et al, 2003).

To run root tubers in the diameter (d) size group 45ï 55 mm, the average height (h) of the knife bed above the belt was set at 40 mm; to run root slices in the size group 55ï 65 mm, h was set at 50 mm; for d between 65 and 75 mm, h was set at 60 mm; for d between 75 and 85mm, h was set at 70 mm; and lastly, for d between 85 and 95 mm, h was set at 80 mm.

The drum speed for the conveyor belt drive was monitored using a phototachometer. In this preliminary experimentation, a drum speed (S) of 100 rpm was used. This is the approximate design speed that will ensure the optimal utilization of the power delivered to the conveyor system by the 2-hp variable speed drive motor. This speed, in turn, gave a linear belt speed (V) of 1.31 m/s. The tensile load, F_s, in each of the 25 sets of springs at each spring-loading point was varied between 44 and 110 N in steps of 22 N. The selection of these loads was informed by the results of an earlier work by Adetan et al (2003) which determined the cassava root peel penetration force per unit length of knife edge.

To acquire data on a root tuber at a given F_s, the experimental peeler was started up. The unpeeled cassava root tuber was fed manually into the machine and onto the top of the conveyor belt at the root pick-up end of the knife assembly. It rolled on its cylindrical surface under the spring-loaded knives on one side and over the conveyor belt on the other side until it was discharged at the other end of the belt peeled. The platform of aluminum sheet (5) over which the belt moved prevented it from sagging

as it conveyed the cassava roots to be peeled under the array of knives set over it. In this way, the knives were kept in close penetration contact with the roots. Using an electronic balance, the mass of each tuber was measured before peeling, after machine peeling and after hand-trimming the machine-peeled tuber. These were recorded as m_1, m_2 and m_3 respectively and subsequently used to calculate the efficiency of peel removal, which is given by Eqn. (1) below.

Adetan et al. (2003) obtained the average percentage by weight of peel in a typical root, p, as 15.1 %. If we define C as the proportion by weight of peel that is removed by the peeler, and R as the proportion of the useful tuber flesh that is recovered after peeling, it can be shown (Adetan, 2002) that

$$C = 1 - \frac{100\,(m_2 - m_3)}{m_1 p} \quad \ldots\ldots (1)$$

and

$$R = \frac{100\,m_3}{m_1(100 - p)} \quad \ldots\ldots (2)$$

where m_1 is the mass of the unpeeled root tuber, m_2 is the mass of the machine-peeled root tuber and m_3 is the mass of the machine-peeled and hand-trimmed root tuber.

An overall peeling quality index, Q, may also be defined as

$$Q = RC \quad \ldots\ldots (3)$$

3. RESULTS AND DISCUSSION

The results of the preliminary tests of the developed experimental peeler are summarized in Table 1. In these preliminary experiments, no useful root flesh was lost. For the different sizes of root slices used in these tests, the useful flesh recovery index obtained in each test was 1. Applying Eqn. (3), the overall peeling quality index, Q, is therefore equal to the peel removal efficiency C in all cases.

Table 1: Results of preliminary machine testing at a linear belt speed of 1.31 m/s

D_1 (mm)	D_2 (mm)	d_3 (mm)	d (mm)	h (mm)	F_s (N)	C	R	Q	C_{av}	State of root after peeling
65	52	45	54	40	44	0.939	1.000	0.939	0.939	Whole
53	53	40	49		66	0.920	1.000	0.920		Whole
59	55	39	51		88	0.973	1.000	0.973		Whole
60	47	21	43		110	0.825	1.000	0.925		Whole
60	64	55	60	50	44	1.000	1.000	1.000	0.988	Whole
67	60	51	59		66	0.953	1.000	0.953		Whole
58	59	59	59		88	1.000	1.000	1.000		Whole
41	65	63	56		110	1.000	1.000	1.000		Whole
62	66	54	61	60.	44	0.323	1.000	0.323	0.638	Whole
85	73	53	70		66	0.679	1.000	0.679		Whole
82	69	42	64		88	0.729	1.000	0.729		Broken
80	72	60	71		110	0.820	1.000	0.820		Whole
73	81	72	75	70	44	0.657	1.000	0.657	0.594	Broken
65	80	63	69		66	0.664	1.000	0.664		Whole
59	80	82	74		88	0.664	1.000	0.664		Whole
72	76	60	69		110	0.392	1.000	0.392		Whole
94	95	79	89	80	44	0.630	1.000	0.630	0.344	Broken
76	87	80	81		66	0.220	1.000	0.220		Whole
69	86	56	70		88	0.152	1.000	0.152		Whole
73	94	55	74		110	0.375	1.000	0.375		Whole

In general, two peeling patterns were observed during the preliminary experiments using the developed peeler. For some of the root slices run in the peeler, peels were finely lacerated by the knives and neatly brushed off the tuber surface. For other roots, the penetrated peels adhered to the knives and unwound from the tuber surface as the tuber rolled on.

Although the preliminary tests of the peeling principle were carried out on slices of root tubers, the results obtained indicate that the developed peeler shows good promise of effectively peeling whole roots of different sizes. The whole roots peeling system may explore the use of several knife assemblies (more than the five available on the present experimental peeler), that are independently spring-loaded and arranged across the knife bed such that the width of the bed will be greater than the possible length of any whole root tuber. Further experimentation and modelling studies on the experimental peeler are expected to yield the optimum conditions for the design of a high efficiency whole roots peeling system, which may be able to eliminate the occurrence of root breakage.

4. CONCLUSIONS

The preponderance of previous cassava peeling research efforts have concentrated on the use of abrasion to remove the peel of cassava roots in a batch peeling system. Success has, however, been limited because small roots become completely grated while larger roots remain largely unpeeled. An experimental peeling machine, which utilises the cassava peeling concept of peel-flesh separation by compression and peel removal by knives, was successfully developed and tested. The following conclusions were drawn from the results of preliminary tests using the peeler:

(i) The developed peeling machine achieves a high efficiency and excellent quality of peeling with virtually no loss of useful tuber flesh.

(ii) For relatively small roots, with diameters less than 65 mm, a peel removal efficiency *C* of approximately 100% was consistently achieved and the peeled roots were never broken. This is a very important improvement over the performance of previous peeling machines.

(iii) The present peeling machine shows promise of overcoming seemingly intractable cassava peeling problems and the limitations of previous abrasive type peelers. Furthermore, based on the peeling concept employed, the present results provide a scientific basis for the development of an efficient whole root peeling system.

REFERENCES

Adetan, D. A. 2002. Modelling of the Mechanical Peeling of Cassava Tubers. Unpublished Ph. D. Thesis, Agricultural Engineering Department, Obafemi Awolowo University, Ile-Ife, Nigeria.

Adetan, D. A., L. O. Adekoya, O. B. Aluko, 2003. Characterisation of Some Properties of Cassava Root Tubers. Journal of Food Engineering. 59: pp 349 ï 353.

Akinrele, I. A., M. I. O. Ero and F. O. Olatunji, 1971. Specifications for Mechanised Processing of Cassava into Gari. F.I.I.R.O. Technical Memorandum Number 26. Lagos, Nigeria.

Ezekwe, G. O., 1979. Mechanizing Cassava Peeling: the PRODA Cassava Nibbling Machine. PRODA Technical Reports 1: pp. 1 ï 20.

Nwokedi, P. M., 1984. Performance of a Cassava Peeling Machine. In Tropical Root Crops Production and Uses in Africa: Proceedings of the 2nd Triennial Symposium of the International Society for Tropical Root Crops, Africa Branch held in Douala, Cameroun, 14 ï 19 August, 1983. pp. 108 ï 110.

Odigboh, E. U., 1976. A Cassava Peeling Machine: Development, Design and Construction. Journal of Agricultural Engineering Research, .21: 361 ï 369.

Odigboh, E. U., 1983. Cassava Production, Processing and Utilization. In Handbook of Tropical Foods (Chan. Jr. H. T., Ed.). Marcel Dekker Inc., New York, Chapter 4, pp. 145 ï 200.

Odigboh, E. U., 1988. Model III Batch Process Cassava Peeling Machine. Paper Presented at the International Conference on Agricultural Engineering, Paris, March 2-8, 1988.

Ohwovoriole, E. N., S. Obi and A. C. C. Mgbeke, 1988. Studies and Preliminary Design for a Cassava Tuber Peeling Machine. Transactions of the ASAE, 31: 380 ï 385.

Suleman, S. O., 1980. The Design and Construction of a Yam Peeler. B.Sc. Project Report, Mechanical Engineering Department, University of Ibadan, Ibadan, Nigeria.

SOME PHYSICAL PROPERTIES OF GROUNDNUTS (*Arachis hypogea L*)

A. F. Alonge[1] and T. A. Adegbulugbe[2]
[1]Dept. of Agricultural Engineering, University of Ilorin, Ilorin, Nigeria
[2]Dept. of Agricultural Engineering, Federal College of Agriculture,
Institute of Agricultural Research & Training, Ibadan, Nigeria.

ABSTRACT

In order to design and fabricate processing and handling equipment for groundnuts (*Arachis Hypogea L.*) some physical properties of shelled and unshelled groundnuts were determined. The mean values of major, minor and intermediate diameter (mutually perpendicular dimensions) were found to be 12.47, 7.21 and 7.78 mm for shelled seeds and 31.19, 10.74 and 10.80 mm for unshelled pods containing two to three seeds. The average sphericity and roundness were found to be 69.61 % and 54.78 % for shelled seeds and 50.17 % and 42 % for unshelled pods. The mean bulk density, porosity, kernel density, volume and angle of repose were found to be 0.60 g/cm^3, 0.46, 1.11 g/cm^3, 0.36 cm^3 and 24.5 degrees respectively for shelled seeds and 0.21 g/cm^3, 0.57 g/cm^3, 0.49 g/cm^3, 1.60 cm^3 and 23.3 degrees for unshelled pods.

KEYWORDS: Physical property, groundnut, shelled pods, unshelled pods, decorticate.

1. INTRODUCTION

Groundnut (*Arachis hypogea* L.), also known as peanut or earthnut, is a member of the *Papilionaical*, the largest and most important of the three divisions of *leguminasae*. Groundnut was cultivated in Peru as far back as about 3000 B. C. from where it was believed to have originated. It was brought to West Africa from Brazil in the 16th century. It comprises of two main types, the first being the bunch or erect type in which the main stem and branches grow upright so that there is little spreading; the nuts are found closed together at the base of the plant. This type is suited to mechanical harvesting. The second is the creeping type with branches trailing along the ground and the plant therefore has spreading habit. Most of the ones grown in West Africa and Nigeria are of the creeping type. Usually after harvesting the crop, they are shelled, decorticated, cleaned before usage either as cake or extraction of the oil for cooking purposes.

To design equipment for shelling and decorticating the groundnuts, their physical properties must be known. Oje and Ugbor (1991), Oje (1993), Koya and Adekoya (1994), Oje et al. (1997), Alonge and Adigun (1999), Adigun and Alonge (2000), Oje et al. (2001), Alonge (2003)) all carried out studies on physical and mechanical properties of some agricultural product. But little is known of the physical properties of groundnut. The purpose of this work was to determine, with sufficient accuracy for design purposes such physical properties as dimensions, weight, angle of repose, coefficient of friction on possible structural surfaces, bulk density, porosity and sphericity of groundnut relevant to its decortication

2. MATERIALS AND METHODS

Ten kilograms of groundnut (shelled and unshelled) used for the experiment were obtained from the Institute of Agricultural Research and Training, Ibadan. The variety used is local, commonly called ñEpa pupaò, an early-maturing type grown in South Western Nigeria. The physical properties determined and the experimental methods are given below:

2.1 Size and Shape

In determining grain size, one hundred each of shelled and unshelled groundnut were randomly selected. Measurements of the three mutually perpendicular axes were made; namely major, intermediate and minor diameters with a micrometer screw gauge

2.2 Weight

This was determined using an electronic balance for 100 seeds.

2.3 Volume and Solids Density

The volume of each seed for one hundred samples was determined by water displacement method as described by Oje and Ugbor (1991). Individual seeds were immersed in water inside a thin tube-measuring cylinder showing a notable rise in water level. The differences in the final and initial readings were recorded as the volume of seed or pod. The density was obtained by dividing weight of seed by its volume. A sinker was used to screen the pod or unshelled groundnut.

2.4 Frontal Area, Sphericity and Roundness

One hundred seeds were each placed in their natural resting position on a sheet of graph paper. A sharp thin pencil was used to carefully trace the edges of the seed. The frontal area was determined by counting the squares within the traced marks. The projected area and the diameters of circle inscribing and circumscribing the projected areas were measured in order to determine the sphericity and roundness based on the following equations:

Roundness = A_P/A_c é é é é é é é é é é é é é (1)

Sphericity = d_i/d_c é é é é é é é é é é é é (2)

where d_c and A_c are the diameter and area of the smallest circumscribing circle respectively while d_i denotes diameter of largest inscribing circle and represents the projected area of the seed.

2.5 Coefficient of Friction and Angle of Repose

The static coefficients of friction of groundnut were determined on three materials plywood, glass and mild steel. A topless and bottomless material box of dimensions 150 mm x 150 mm x 40 mm was filled with the seeds and placed on adjustable tilting table onto which the material to be tested has previously been fastened. The box was placed on one end of the surface and raised slightly so it was not touching the material. A screw device slowly tilted to the table until the friction force between the seeds and the material was overcome by gravity and movement down the slope began. The angle of inclination was read from a graduated protractor attached to the tilting table. Five replications were carried out for shelled seeds and unshelled pods.

According to Mohsenin (1978) and Chakraverty (1988), the tangent of the angle of inclination is the static coefficient of friction of the grain on the material. Oje and Ugbor (1991) determined static coefficient of friction for different surfaces such as galvanized steel, plywood and glass. They also described the determination of angle of repose by using a specially constructed box with the crop with a removable front panel. The box is filled with the crop, then the front panel is quickly removed. This allows the grain to flow to its natural slope. This slope is a measure of angle of repose. This method was used for the experiment.

2.6 Bulk Density

The bulk density was determined by weighing a $100cm^3$ cylinder empty. The cylinder was then filled with the seeds and reweighed.

$$D_b = \frac{M_2 - M_1}{V} \quad \text{.....(3)}$$

where D_b is bulk density, M_1 is the mass of empty cylinder, M_2 is mass of cylinder plus seeds and V is the volume of cylinder. Five trials were carried out for each set of seed and their means were recorded.

2.7 Porosity

Based on the relationship for porosity by Mohsehnin (1978) the porosity was calculated thus:
where P_f is the porosity of grain, D_b is the bulk density and D_s is the solid or kernel density of grain.

$$P_f = 1 - \frac{D_b}{D_s} \quad \text{.....(4)}$$

3. RESULTS AND DISCUSSION

The summary of the results for all the properties measured is shown in Tables 1 and 2 for shelled seeds and unshelled pods respectively. The frequency distribution of some of the properties is shown in Figures 1 and 2 for shelled seeds and unshelled groundnut pods. For shelled seeds, sixty percent of the major axes fall between 12 and 13 mm, 94% of the intermediate axes falls between 6.7 mm and 9 mm and 94 % of the minor axes falls between 6.5 mm and 8 mm. For the unshelled pods 82 % of major diameter falls between 20 mm and 35 mm, 78 % of intermediate diameter falls between 9.5 mm to 11.5 mm while 80 % of minor diameter falls between 9.5 mm to 10 mm. The frequency distribution curve for major and intermediate axes skewed towards the right while for the minor axes it is near normal. These properties are needed in designing diameter of sieves for sieve cleaner.

The density of the shelled groundnut falls between 1.02 and 1.27 g/cm^3. This implies that the seeds will sink in water, which makes it possible to separate them from other materials that are less dense than water. The frequency distribution for density of the unshelled groundnut is close to normal. It varies between 0.40 g/cm^3 and 0.58 g/cm^3, the mean being 0.49 g/cm^3. Separation from unwanted material denser than water is possible for example stones. The mean porosity obtained for the shelled groundnut was 0.46 and 0.57 for the unshelled. This shows that a pack of unshelled groundnut pods is more porous than the shelled one. This property is required in air and heat flow in an agricultural material. This shows how easily a stream of heated air for drying will pass through a pack of material and thus affect the rate of drying of the materials. From this result, unshelled groundnut pods might dry faster than shelled seeds during air drying process.

With regards to the static coefficient of friction for shelled groundnut determined on the three structural surfaces it was found that, glass surface had the highest mean value of 0.535 while the lowest value was by mild steel was 0.455. For the unshelled pods the plywood has the highest mean value of 0.52 while the lowest value was on glass with a mean value of 0.495. This property is needed in the design of agricultural machine hopper and other conveying equipment. It determines how a pack of grain or seed will flow in these systems.

The angle of repose for shelled seeds was found to be between 22^0 and 27^0, while for the unshelled pods it was between 27^0 and 30^0. This property determines the minimum slope of flow in self-emptying bin or minimum slope of flow in a hopper. The mean frontal or projected area for the shelled is 68.8 mm^2, for the unshelled pod it is 309.2 mm^2. This property affects the velocity of air stream that can be used in order to separate the seed from unwanted material in pneumatic separator or to convey seed in pneumatic conveying.

The highest roundness value obtained for unshelled pods was 58.93 % while the highest sphericity value obtained was 74.78 % for unshelled groundnut shown in Table 2. This implies that the tendency for the material to roll is fairly high. For the shelled seed the highest roundness value obtained was 64.79 % while the highest sphericity value obtained was 85.49. This shows that the material will always tend to roll when it is on a particular orientation. This property is always considered when designing hopper and dehulling equipment for seeds.

Table 1: Some physical properties of shelled groundnut

	No. of observations	Mini Value	Mean Value	Maxi Value	Standard Deviation
Major Diameter (cm)	100	6.71	12.27	15.71	1.92
Intermediate Diameter (cm)	100	6.79	7.78	8.92	0.51
Minor Diameter (cm)	100	5.54	7.21	9.30	0.68
Weight (g)	100	0.29	0.40	0.54	0.06
Geometric Mean diameter (cm)	100	6.96	8.84	10.37	0.67
Roundness	100	49.12	54.73	64.79	6.12
Sphericity (%)	100	61.74	69.61	85.49	4.78
Volume (cm^3)	100	0.25	0.36	0.45	0.06
Solid Density (g/cm^3)	100	1.02	1.11	1.27	0.06
Bulk Density (g/cm^3)	5	0.59	0.60	0.61	0.01
Surface Area (mm^2)	100	600.27	628.91	650.77	19.25
Porosity	5	0.42	0.46	0.52	0.02
Frontal Area (mm^2)	100	58.00	68.80	82.00	9.24
Repose Angle (degrees)	5	22	24.50	27.00	2.07
Coefficient of friction on					
(i) Plywood	11	0.47	0.525	0.58	0.05
(ii) Mild steel	11	0.42	0.455	0.49	0.04
(iii) Glass	11	0.45	0.535	0.62	0.07

Table 2: Some physical properties of unshelled groundnut pods

	No. of observations	Mini Value	Mean Value	Maxi Value	Standard Deviation
Major Diameter (cm)	100	16.29	31.19	41.94	5.16
Intermediate diameter (cm)	100	8.59	10.80	12.23	0.81
Minor Diameter (cm)	100	9.23	10.74	12.51	0.75
Weight (g)	100	0.40	1.25	1.94	0.38
Geometric Mean diameter (cm)	100	12.00	15.28	17.70	1.23
Roundness	100	19.12	42.2	58.93	15.43
Sphericity (%)	100	40.40	50.17	74.78	6.66
Volume (cm^3)	100	1.50	1.60	3.50	0.82
Density (g/cm^3)	100	0.40	0.49	0.58	0.07
Bulk Density (g/cm^3)	5	0.19	0.21	0.23	0.01
Surface Area (mm^2)	100	40.38	46.27	52.16	16.13
Porosity	5	0.53	0.57	0.60	0.02
Frontal Area (mm^2)	100	248	273	298	82.56
Repose Angle (degrees)	5	27.0	28.5	30.0	1.20
Coefficient of friction on					
(i) Plywood	11	0.47	0.520	0.57	0.03
(ii) Glass	11	0.45	0.470	0.49	0.01
(iii) Mild steel	11	0.48	0.495	0.51	0.02

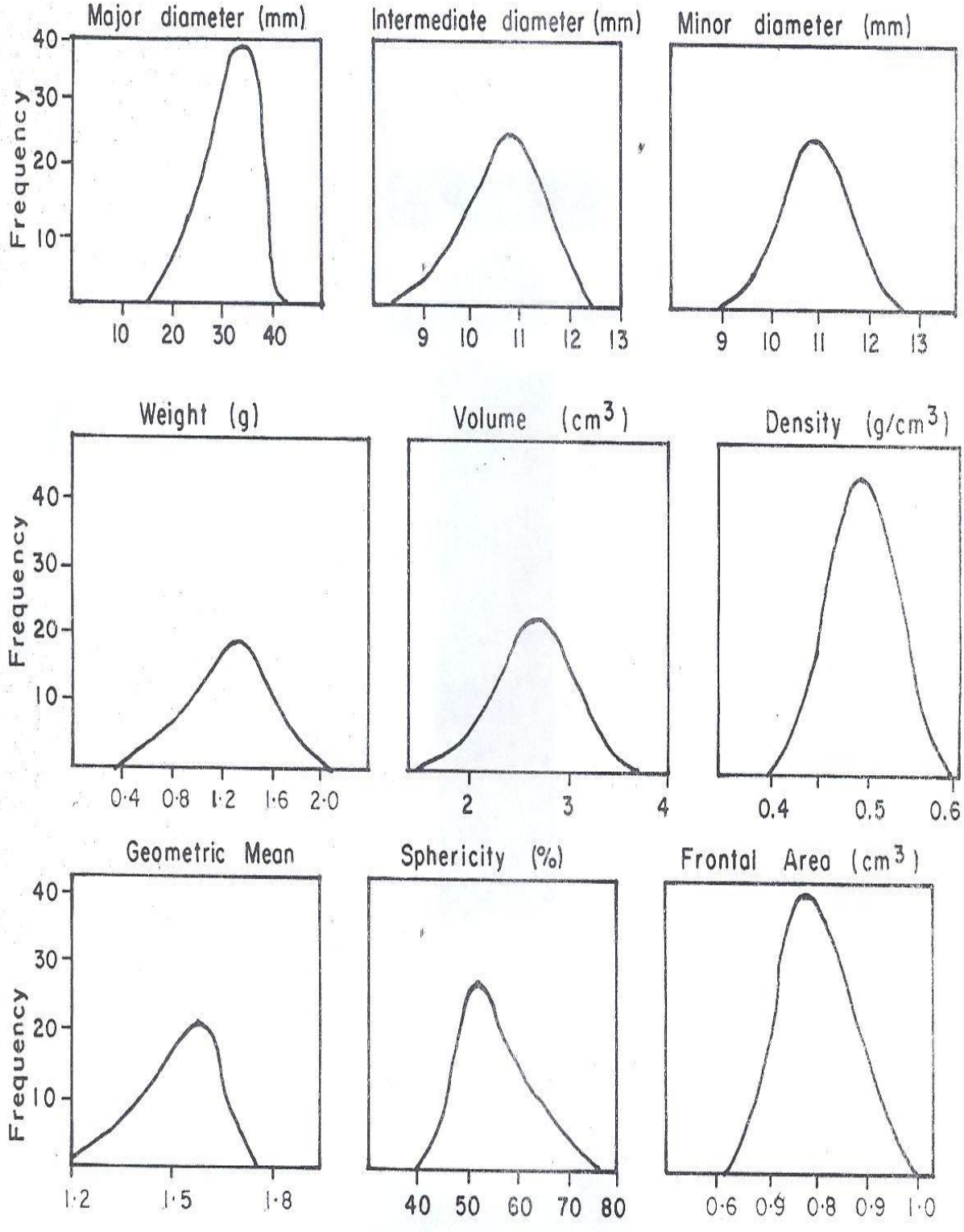


Fig. 1: Frequency distribution of some physical properties of unshelled groundnut pods.

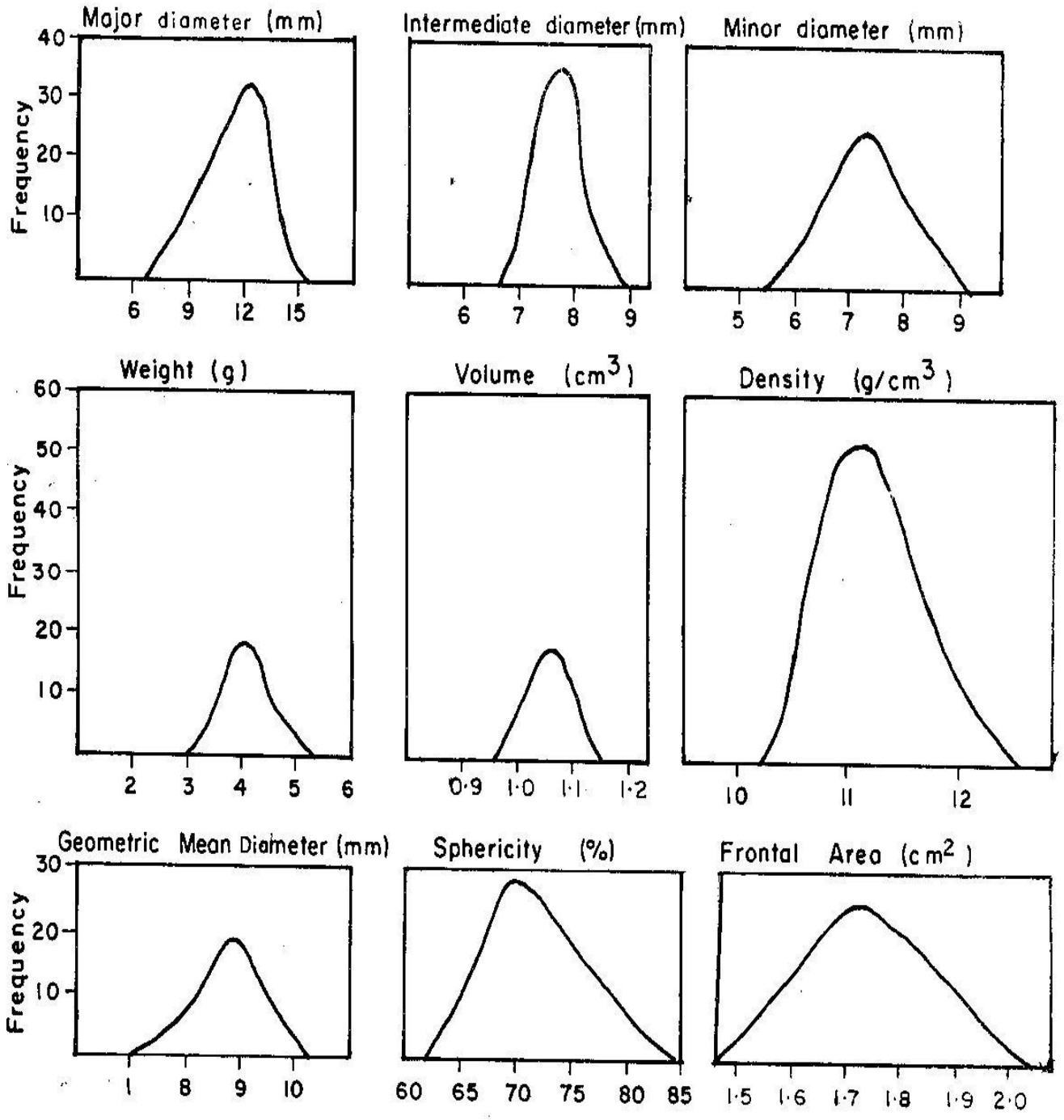


Fig. 2: Frequency distribution of some physical properties of shelled groundnut pods

4. CONCLUSIONS

The physical properties of groundnut (shelled and unshelled) were measured. The following conclusions are drawn:

(a) For shelled seeds - The estimated mean major, minor and intermediate diameters were found to be 12.49 mm. 7.21 mm and 7.28 mm respectively. The roundness was found to be 69.61 % while the sphericity was 54.76 %. The mean weight was found to be 0.40g.

(b) For unshelled pods ï The estimated mean diameter for major, minor and intermediate axes were found to be 312.19 mm, 10.80 mm and 10.74 mm respectively. The roundness was 50.17 % while sphericity was 42.2 %. The average weight was found to be 1.25g.

(c) The results for the coefficient of friction for both shelled and unshelled groundnut showed that hopper and unloading device need not be built very steeply.

ACKNOWLEDGEMENT

The authors hereby acknowledge the contributions of Areo, B. O. and Taiwo, A. A in data collection and the assistance given during the experiment.

REFERENCES

Adigun, Y. J and Alonge, A. F. 2000 Physical and rheological properties of *Prosopis Africana* pods relevant to their dehulling. Nigerian Journal of Technology (NIJOTECH), 19(1):52-58.

Alonge, A. F. 2003. The Effect of Moisture Content on Mechanical Properties of Soybean (Glycine max (L) Merr.). Journal of Agricultural Research and Development (JARD), 2: 60-69.

Alonge, A. F. and Adigun, Y. J. 1999. Some physical and aerodynamic properties of sorghum as relate to cleaning. Nigerian Journal of Pure and Applied Sciences. 14: 992-998.

Charkraverty, A. 1988. Post Harvest Technology of Cereals, Pulse and Oil seeds. Revised Edition Oxford and IBH Publishing Co. Ltd., New Delhi. pgs 60 ï 165.

Koya, O. A. and Adekoya, L. O. 1994. Some physical and aerodynamic properties of grain crops relevant to destoning. Ife Journal of Technology.4(2):35-40

Mohsenin, N. N. 1978. Physical properties of Plant and Animal Materials, New York: Gordon and Breach Publishers.

Oje, K. 1993. Locust bean Pods and Seeds: some physical properties of relevance to dehulling and seed processing. Journal of Food Science and Technology 30(4): 253-255.

Oje, K, Alonge, A. F and Adigun, Y. J. 1997. Variation in Physical properties of Melon Seeds at its different moisture level. Journal of Food Science and Technology (JFST), Mysore, India. 36(1): 42-45.

Oje, K, Alonge, A. F and Adigun, Y. J. 2001: Some engineering properties of Shea Nut relevant to mechanical processing. Ife Journal of Technology (IJT). 10(2):17 - 20.

Oje, K. and Ugbor, E. C. 1991. Some physical properties of Oilbean seed. Journal of Agricultural Engineering Research. 50:305-313.

DEVELOPMENT AND PERFORMANCE EVALUATION OF A POULTRY FEED MIXER

L. Gbadamosi and S. A.Magaji
Department of Agricultural Engineering and Water Resources
Institute of Technology, Kwara State Polytechnic, Ilorin.

ABSTRACT

A poultry feed mixer was designed, constructed and evaluated for its performance. The effectiveness of mixing was based on the value of standard deviation and coefficient of variation of the sample collected from the tested mixed materials at the operating speeds. The performance of the mixer at the tested operating speeds of 100rpm, 150rpm 250rpm were: standard deviation, (S.D) 7.37 and coefficient of variation (CV) 19.33%; S.D. 1.29 and CV 3.07% and SD of 10.84 and CV of 46.98% respectively. The effectiveness of mixing of the mixer was high at operating speed of 150rpm, followed by operating speed of 100rpm but the effectiveness of mixing of the mixer was lowest at operating speed of 250rpm.

KEYWORDS: Poultry, feed mixer, standard deviation, coefficient of variation, livestock feeds.

1. INTRODUCTION

Livestock feed is the general term for food given to farm animals. The regular supply of food to farm animals is very essential to a healthy and productive life. Feed is an essential requirement in poultry production as it is in all other livestock keeping. Oluyemi and Robert (1978) stated that once the poultry man has selected a good bird with long life ability, high genetic capacity to grow or lay eggs effectively and has prepared the housing and the management essential for the successful operation, the next thing is to produce the most efficient nutritionally complete diet to suit a particular environmental condition.

Livestock feed as a prominent factor in poultry production influences significantly the overall quality and quantity of birds and feeds. Preparation involves grinding and mixing different ingredients to form homogeneous mix (Davis and Hall, 1979).

Mixing as one of the processes involved in feed preparation must be attended to with care as improper mixing of feed ingredients could produce unbalance ration that undernourishes the birds. Smith and Wilkes, (1984) and Beldin et. al (1968) reported the need to use mixer when attempting to mix two or more ground feeds of known feeding value to obtain a balance ration as it ensures mixes of uniform consistency. However, most of the available mixers currently in the market are imported, sophisticated in design and very expensive for rural farmers to afford and maintain. There is a need for a small sized, simple and inexpensive mixer that would solve the problem of providing an alternative feed mix for rural livestock farmers.

The aim of this paper is to develop and evaluate the performance of such a poultry feed mixer.

2. DEVELOPMENT OF THE POULTRY FEED MIXER

2.1 Background

Mixers are classified according to their method of mixing. Solid particles are mixed by the different methods as reported by Lacey (1984). Convective mixing, occurs by the transportation of group of particles from one location of the mixer to another location. Diffuse mixing, involves the distribution of particles over a freshly developed surface of the materials. Shear mixing involves the setting up of slip planes within the mixture.

Beldin et. al (1968) classified mixing into different categories. These include layer mixing, which is the mixing of ingredients in layers in a feeding wagon. It occurs as different layers move through the beaters and fall into the cross conveyors. Stream mixing is a form of layer mixing on a more refined scale in which accurately metered

amount of feed are deposited onto a moving conveyor with each cross section of feed containing exactly the required amounts of each of the different ingredients. Batch mixing involves mixing which take place in the tank of the mixer in batch quantities by means of re-circulation process. The action of the mixing mechanism is such that feed elements are recirculated at different speed than the others.

Feed mixers designers and farmers have use different methods as reported by Beldin et. al (1968) to determine the quality of feed mix. Firstly, visual observation and comparison where farmers closely observe the feed while it is being unloaded in bunks and semi-feeders, and note the feed for uniform mix. Secondly, noting uniform condition of the livestock, where farmers watch the condition of the herds as a measure of mixing ability of the mixer. The lesser the trouble with the cattle the better the mixer. Thirdly, addition of an easily distinguishable tracer and visually observing the overall uniformity distribution is a method where coloured tracers are added to the mix and the uniformity of the tracers distribution is noted. The fourth method is laboratory analysis of samples where mixed feeds are sent to the public or commercial laboratories for overall ration analysis.

The factors affecting the throughput of the auger conveyor according to Stevens (1962) include operating speed, elevation of the auger conveyor and the pitch of the auger. The peak throughput based on the experiment performed on an auger conveyor was attained when the operating speed was in the region of 100rpm, but commercial auger in common use run at speed range between 1000rpm and 2000rpm for a 3inch diameter (76.2mm)-auger and 600 to 750 rpm for a 6inch (152.4mm) auger. As the elevation of the conveyor increases, the throughput decreases except the auger with the smallest value of ratio of pitch to the diameter. Most commercial augers have a value ratio of pitch to diameter of approximately 1, and high capacity conveyor of free flowing materials has a value ratio of pitch to diameter of approximately 1.5.

2.2 Design Consideration

In designing the mixer, the following factors were considered:

-Material Selection; minimum cost, strength, durability, appearance and availability of local materials.
-Stability of the Machine; geometrical shape of the mixer as well as the strength of the materials that would withstand vibrations under different operating conditions.
-Power Requirements; estimation of the total power considers the power to operate the mixer empty and the power to operate it at a desired load and desired elevation.
-Machine Capacity; economic utilization of the feed based on the population of the birds and cost of the feed materials.

2.3 Description of Poultry Feed Mixer

A vertical mixer was designed and constructed. The mixer comprises of the following components as shown in Figures 1 and 2. The major components include: the main body of total volume of $0.1852m^3$ and was constructed of a sheet metal of gauge 20. The hopper is right angle triangle in shape and has a volume of $0.01125m^3$. The auger conveyor is a hollow shaft with external diameter of 50mm and internal diameter of 44mm and pitch of 160mm. The capacity of the auger conveyor was 1.56tonnes/hr determined from the expression of Stevens (1962). The bearing was rolling contact bearing (single row, deep groove ball bearing). The bearing was chosen according to ASAE standard as given by Hall, et al, (1988). The power requirements consist of the power to run the mixer empty and the power to run the mixer on load. The total power required is 3.80kW or 5hp. The belt chosen is V-belt, rubber impregnated with leather of length 840mm.

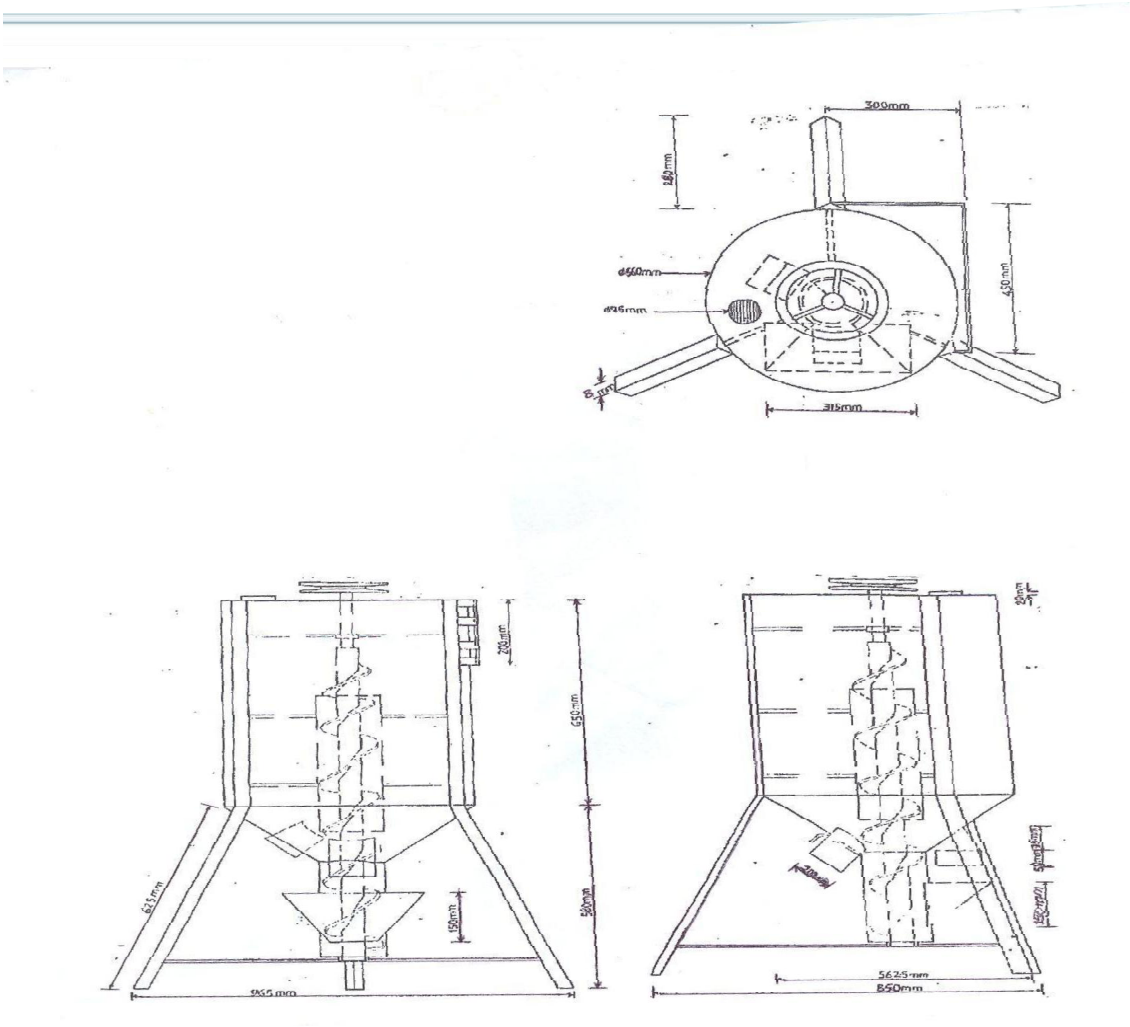


Fig. 1. Details of the poultry mixer



Fig. 2. Picture of a poultry mixer

The machine was developed and constructed as a vertical mixer. The mixer works by the principle of convectional mixing. The mixer is fed from the hopper and can be operated by an electric motor of 5hp. The mixing starts with the charging of a desired proportions of feed ingredients via the hopper into the mixer which is simultaneously followed by addition of additives. The mixer is allowed to run for a period of time to effect proper mixing of the feed ingredients. The mechanism of mixing involves the conveyance of feed materials from the lower part to the upper part of mixer by the auger conveyor working at the desired operating speed.

The materials on getting to the upper part sprinkles on the mixer parts and get down by gravity. The process repeats until the desired mixing is obtained by viewing the degree of mixing in the testing spout of the mixer.

2.4 Performance Evaluation

The test procedure followed that of Beldin, et al. (1968). Three operating speeds, of 100rpm, 150rpm 250rpm were used for the performance test. As the mixer is working, 4kg of ground corn mixed with 1kg of soyabean seeds serving as local tracer were fed into the mixer via the hopper. The mixer was operated for five minutes for each of the three operating speeds, and the time was measured using stop-watch. After mixing and from the mixed feed, an equally spaced 13 samples measuring 100gm per sample were randomly taken. The soyabean seeds contained in every samples were sorted and counted. The effectiveness of mixing of the mixer was calculated as coefficient of variation from the relationship:

$$CV = \frac{SD}{m} * 100\% \quad \text{----------(1)}$$

Where, SD = standard Deviation of mixed feeds and is mathematically expressed as

$$SD = \frac{\tilde{a} \times (x-m)^2}{n} \quad \text{----------(2)}$$

m = mean of soyabeans seeds distribution in the samples; and is mathematically expressed as,

$$m = \frac{\times x}{n} \quad \text{----------(3)}$$

Where: x = the number of soyabeans seeds in the sample, n = number of samples collected.

3. RESULTS AND DISCUSSION

The result of the performance evaluation of the poultry feed mixer are as shown in Table 1 and Table 2. It is seen from Table 2 that the standard deviation (SD) and the coefficient of variation (CV) are high at operating speed of 100rpm and higher at operating speed of 250rpm but low at operating speed of 150rpm. The low value of SD and CV is an indication of uniform distribution of the soyabeans seeds (local tracer) in the tested mixed feed, and the high value of SD and CV is an indication of non-uniform distribution and the higher value of SD and CV is an indication of poor distribution of the local tracer on the tested samples (Beldin, et. al, 1968). The effectiveness of mixing of the mixer could be considered high at the operating speed of 150rpm, followed by the operating speed of 100rpm but considered low at operating speed of 250rpm.

Table 1. Performance test result of the poultry feed mixer

.

Sample No.	100rpm % of Soyabeans seeds in the sample (x)	100rpm $(x-m)^2$	150rpm % of Soyabeans seeds in the sample (x)	150rpm $(x-m)^2$	250rpm % of Soyabeans seeds in the sample (x)	250rpm $(x-m)^2$
1	40	3.42	42	0	20	9.42
2	36	4.41	40	4	40	286.62
3	30	66.42	43	1	10	170.82
4	32	37.82	40	4	25	3.72
5	42	14.82	42	0	15	65.12
6	50	140.42	43	1	5	326.52
7	34	17.22	42	0	10	170.82
8	48	97.02	42	0	20	9.42
9	46	61.62	43	1	25	3.72
10	24	200.22	44	4	30	48.02
11	36	4.62	43	1	25	3.72
12	38	0.023	42	0	40	170.82
13	40	3.423	40	4	35	142.32
Total	416	651.456	546	20	300	1411.06

Table 2. Summary of the performance test results of the mixer

Speed of operation (PM)	100	150	250
No. Sample Collected	13	13	13
Mean Value of the Samples	38.15	42	23.07
SD	7.37	1.29	10.98
CV (%)	19.30	3.07	46.98

4. CONCLUSION

The poultry feed mixer was designed, constructed and evaluated. It was concluded that the effectiveness of mixing is high at moderate operating speed. The mixer performance was high at operating speed of 150rpm with standard deviation (SD) and the coefficient of variation (CV) of 1.29 and 3.07% respectively.

REFERENCES

Beldin, R. L. Klouda, A. E. and Lindstrom, H. R. 1968. Farm Feed Mixer Evaluation, Transaction of the ASAE, pp 771-775.

Davis, D. C. and Hall, C. W. 1979. Processing Equipment for Agricultural Products, 2nd Edition, AUI Publishing Company, London pp. 1 and 29.

Hall, H; Holowenko, M. S. and Herman, G L. 1988. Theory and Problems of Machine Design, Schaum Outline Series, MacGraw-Hill Book Company, New York.

Lacey, P. M. 1984. Development in the Theory of Particles Mixings, Journal of Chemical Engineering, Vol. 4., pp 257.

Oluyemi, J. A. and Robert, F. A. 1978. Poultry Production in Warm Wet Climates, Macmillan Press Publishers, Hongkong, pp 133-137.

Smith, A. E. and Wilkes, M. S. 1984. Farm Machinery and Equipment, 4th Edition, McGraw-Hill Publishing Company Ltd. Pp. 374-375.

Steven, G. N. 1962. Performance Tests on Experimental Auger Conveyor. Journal of Agricultural Engineering Research.

MODELING THE CHANGES IN SIZE OF AIR-BORNE LIQUID SPRAY DROPLETS IN WINDY AND STILL AIR CONDITIONS

S. I. Oluka[1], C. O. Akubuo[2] and E. U. Odigboh[3]
[1] Dept of Agricultural and Bioresource Engineering, Enugu State University of Science and Technology, Enugu, Nigeria
[2, 3] Dept of Agricultural and Bioresource Engineering, University of Nigeria, Nsukka-Nigeria.

ABSTRACT

Mathematical models considering the aerodynamic and physical characteristics of liquid spray droplets as well as the transport properties of air were developed to simulate changes in the size of air-borne liquid spray droplets under varying field conditions. The models were programmed for solutions using the fourth order Runge Kuta numerical integration techniques. A wind tunnel was constructed to provide an experimental base for the validation of the mathematical models.

The model predicted a percentage size decrease of 11.6, 10.78, 9.09 and 7.758 % at still air and 29.52, 19.86, 14.99 and 12.04 % at the wind speed of 1.0 m/s for droplet sizes of 100, 150, 200 and 250 microns respectively after 10 seconds of being air-borne. As the size reduction rate in air increases, the chances of off-target deposition of the spray droplets increase. The results of the numerical computations compare fairly well with validation results confirming that the rate of change in the size of an air-borne liquid spray droplet is influenced by the droplet size, droplet retention time in air, wind velocity and intensity.

KEYWORDS: Modeling, change in size, air-borne, liquid, spray, droplet.

1. INTRODUCTION

In agriculture, agro-chemicals are used to protect crops against insects, weeds, and diseases. One popular method of doing this is by spraying. Whenever a liquid spray droplet is exposed to any environment of less than 100% relative humidity, the droplet will undergo a reduction in size by the net mass transfer of the water molecules in vapor state (Law and Bowen, 1975). The size reduction process, induced by such factors as the environment, aerodynamic and physical characteristics of the spray droplet, transport properties of the transport medium (air) and droplet fluid (water), influence the degree of off-target or on-target deposition of the spray droplets. Off- target deposition of agrochemicals causes not only wastage of costly chemicals, but also environmental pollution of nearby crops, as well as air, soil and water resources around the farm.

There is the need therefore to understand the interaction of the various factors affecting the size reduction processes of liquid spray droplets in dynamic conditions. One of the ways of achieving this understanding is by mathematical modeling and computer based simulation.

Previous attempts at developing mathematical models for simulating the reduction in size of spray droplets have been made (Law and Bowen, 1975, Goering et al, 1972, Williamson and Thread gill 1974 and Miller and Hadfield 1989). From review of the literature, it was seen that no single model has been able to incorporate most of the parameters influencing the reduction in size of liquid droplets in air. For instance while some of the researchers view spray droplet evaporation as being closely related only to convection of heat from bodies of the same shape; others see it as solely a molecular diffusion problem. These different understandings of the problem led to the development of different models some of which vary very significantly (Miller and Hadfield 1989).

The objective of this study was to develop and validate a simulation model which will consider all the various factors of the environment, physical, aerodynamic and external factors affecting the size reduction and deposition of an air-borne liquid droplet. Such a model will provide an insight into the dynamics and deposition of an air-borne spray droplet thereby supplying the required environmental,

physical and aerodynamic data for maximizing efficient spray droplet deposition and minimizing drift under varying spraying conditions.

2. MATERIALS AND METHODS

2.1 Model Development

In developing the model, the basic principles from the earlier works were applied (Marshall, 1955; Ranz and Marshall 1952; Williamson and Thread gill 1974; Goering et al, 1972 and Marchant,1977.

Earlier studies on air-borne evaporation of spray droplets resulting to size reduction (Ranz and Marshall 1952), reported that the rate of change of mass of an air-borne spray droplet was strongly related to the surface area of the droplet in air, the mass transfer coefficient of the droplet, the flow regime and the vapor pressure difference between the ambient air and the evaporating droplet surface. They mathematically expressed these relationships as follows:

$\partial m / \partial t = K_g . A_s . \Delta P . M_p$ é 1

Where $\partial m / \partial t$ = mass transfer rate (gs^{-1})
K_g = Mass transfer coefficient (moles $s^{-1}m^{-2}$)
M_p = Molecular weight of the droplet liquid (g $mole^{-1}$)
A_s =Area of mass transfer = total surface area of droplet (m^2)
ΔP = Vapor pressure difference (gm^{-1} s^{-2})

Assuming that the droplets are spherical in shape (Smith et al., 1982; Braig 1986; Goering et al, 1972), then we obtain,

$A_s = \pi D_p / 4$ and $V_s = 4\pi r^3 / 3$

A_s = Area of the spherical spray droplet (m^2)
V_s =volume of sphere (m^3)
D_p=diameter of sphere (m)
r = radius of the sphere (m)

From the relationship: density = mass/ volume, we have
Mass = density x volume
= ρ_p x volume of sphere.
$M = \rho_p \pi D_p^3 / 6$ é é é é é é é é é é é é é é é é é é é .2

Where M= mass of droplet liquid (g)
ρ_p=density of liquid (gm^{-3})
Differentiating equation 2 with respect to D_p, we have,

$\partial m / \partial t = \rho_p \pi D_p^2 / 2 * \partial D_p / \partial t$é é é é é é é é é é é é é ..3

Comparing equations 1 and 3, we have,

$= \rho_p \pi D_p^2 / 2 * \partial D_P / \partial t = K_g * A_s * \Delta P * M$é é é é é é é é é é .4

The density of fluid (air), droplet diameter, diffusivity and the flow regime of the droplet in air influence the mass transfer coefficient, K_g. Hence K_g could be expressed as

$K_g = \rho_a * D_v * N_N / M_a * D_p * P_a$ é é é é é é é é é é é é é é 5

Where ρ_a = density of air (kgm^{-3})
D_v = diffusivity of the droplet vapor in air (m^2s^{-1})
N_N= Nusselt Number of heat and mass transfer (dimensionless)
M_a = Molecular weight of the fluid (air) ($g\ mole^{-1}$)
D_p= droplet or particle diameter (m)
P_a = Partial pressure of air ($g\ m^{-1}s^{-2}$)

$$N_N = 2.0 + 0.6\ (RN)^{1/2}\ (SN)^{1/3} \quad \text{é é é é é é é é é é é é é é é 6}$$

Therefore arranging equations 5 and 6 gives

$$K_g = (\rho_a D_v / M_a D_p P_a)\ [2.0 + 0.6\ (RN)^{1/2}\ (SN)^{1/3}] \quad \text{é é é é .7}$$

Substituting equation 7 into 4, we obtain,

$$\rho_p \pi D_p^2/2 * \partial D_p/\partial t = (\rho_a D_v/ M_a D_p P_a)\ [2.0 + 0.6\ (RN)^{1/2}\ (SN)^{1/3}]\ (\pi D_p^2/ 4 * \Delta P * M_p) \quad \text{é .8}$$

Simplifying equation 8 gives

$$\partial D_p/\partial t = -(\rho_a D_v.M_p\ \Delta P / 2 * M_a.D_p.P_a.\rho_p)\ [2.0 + 0.6\ (RN)^{1/2}\ (SN)^{1/3}] \quad \text{é é é ..9}$$

The negative sign indicates that the air borne droplet is reducing in size.

From previous work (Marshall, 1955)

$$\partial Dp/\partial t = 8\Delta TK/\rho_p.\delta \quad \text{é 10}$$

Where ΔT = temperature difference between air and droplet surface (^oC)
K = average thermal conductivity of gas film surrounding the droplet ($KW\ m^{-1}\ K^{-1)}$
ρ_p =density of the droplet liquid ($g\ m^{-1}$)
δ = latent heat of vaporization ($KW\ kg^{-1}$)

From equations 9 and 10, we have,

$$\partial D_p/\partial t = 8\Delta TK/\rho_p.\delta = (\rho_a D_v.M_p\ \Delta P / 2.M_a.D_p.P_a.\rho_p)\ [2.0 + 0.6(RN)^{1/2}(SN)^{1/3} \quad \text{é ¨11}$$

Simplifying and rearranging equation 11, gives

$$\partial D_p/\partial t = (\rho_a.D_v.M_p\ \Delta P.\delta / 8 * M_a.D_p.P_a.\ \Delta T.K)\ [1 + 0.3\ (RN)^{1/2}\ (SN)^{1/3}] \quad \text{é é é .12}$$

Where RN = Reynolds Number (dimensionless)
SN = Schmidt Number (dimensionless)
Other parameters as earlier defined.

Equation 12 gives the complete mathematical model for describing the rate of change of size of any air borne water based spray droplet in any environment where the relative humidity is less than 100%.

2.2 Wind Effect

During, unstable atmosphere like that of windy environment often experienced during field spraying operations, an air borne spray droplet tends to be drifted horizontally or vertically down to the target or off-target.

In order to predict what happens to the droplet along the horizontal and vertical directions of motion of the droplet, it is assumed that the droplet moves with an initial velocity V_o, direction ϕ, relative to the horizontal and time, t. Wind with velocity, V_a, blows on the droplet at an angle α, relative to the horizontal as shown in Fig. 1.

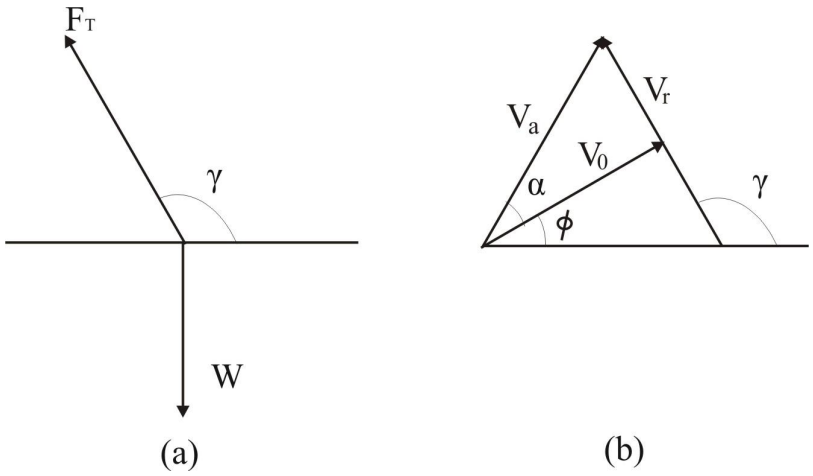


Figure 1.0: (a) Forces acting on the droplet. (b) Velocity diagram

Analysis of figure 1.0 results to equations 13 and 14

$$\sum (RH) = V_a \cos\breve{U} + V_o \cos\phi \quad \text{.....13}$$

$$\sum (RV) = V_a \sin\breve{U} + V_o \sin\phi \quad \text{é é é é é é é é é é é é é é é é ..14}$$

Where RH = component of the air and droplet velocities along the horizontal direction.
RV = component of the air and droplet velocities along the vertical direction.

2.3 The Model

The evaporation rate of an air-borne spray droplet is directly proportional to the velocities of the droplet liquid and its medium (air) (Sutton, 1953).
Therefore,

$$\lambda \quad \text{Ð } (V_a + V_o)$$

$$\lambda = k\,(V_a + V_o) \quad \text{é ..15}$$

Where λ = evaporation rate for water based droplet, K = factors of evaporation, V_a= velocity of air. V_o = initial velocity of the droplet.

Comparing and arranging equations 12, 13 and 14 with 15 gives

$$\partial D_p\,(x)/\partial t = -1/8\,(\rho_a . D_v . M_p . \Delta P . \delta\ /^* M_a . D_p . P_a .\ \Delta T . K)\,(1 + 0.3\,(RN)^{1/2}\,(SN)^{1/3})\ RH\text{é}\ \ 16$$

$\partial D_p (y)/\partial t = -1/8 (\rho_a.D_v.M_p \Delta P.\delta / *M_a.D_p.P_a.\Delta T.K) (1 + 0.3 (RN)^{1/2} (SN)^{1/3})$ RVé 17

Where $\partial D_p (x)/\partial t$ = droplet evaporation rate in the horizontal direction. $\partial D_p (y)/\partial t$ = droplet evaporation rate in the vertical direction.

Equations 16 and 17 were used to simulate spray droplet evaporation along the horizontal and vertical directions of wind motion, respectively.

2.4 Numerical Solution

The set of equations 1-17 represents the set of mathematical models used to predict the evaporation of an air-borne spray water-based droplet. The equations were programmed for solutions using 4th order Runge Kuta numerical integration technique.

Fourth Order Runge Kutta numerical method was used in solving the set of equations. The equations were first reduced to a system of first-order equations and then solved simultaneously. The advantage of this method is that as the X, Y locations of the droplet are changing with time, so also is the droplet diameter which is decreasing through evaporation. Thus, at every discrete step, the droplet diameter is updated to get the new location.

The fourth-order Runge-kutta algorithm for the one-step integration of a single first-order equation with one appropriate initial condition was written for a system of n-first order equations with n-initial conditions as presented below.

For a system of n equations:

ÖΠ_1/Ö= $f_1(t, Y_1, Y_2,.., Y_n)$
ÖY_2/Ö=$f_2 (t, Y_1, Y_2,..,Y_n)$
ÖY_n/Ö=$f_3 (t,Y_1,Y_2,$é $,Y_n)$
The one-step integration across the ith interval is:
$Y_{j,i+1}=Y_{ji}+h\Phi_j$
$=y_{ji}+h (k_{ji}+2k_{j2}+2k_{j3}+k_{j4})/6$
Where:
$K_{ji}=f_j (t_i, y_{1i}, y_{2i},$é $, y_{ni})$
$k_{j2}=f_j (t_i+½h, y_{1i}, y_{2i},.$é $y_{ni})$
$k_{j3}=f_j (x_i + ½ h, y_{1i}, y_{2i},$é*, y_{ni}, *)
$k_{j4}=f_j (x_i + h, y_{1i}, y_{2i},$é $y_{ni},)$
* * *

2.5 Model Validation

Results of the numerical computations were compared with experimental results obtained during a series of model validation tests under the controlled environmental conditions of a wind tunnel facility.

The wind tunnel was constructed to provide an experimental base for the validation of the mathematical model. The tests were carried out inside the test chamber of the wind tunnel at different heights, wind velocity and time intervals. The spray droplets were generated using a knapsack sprayer and were collected at different equidistant positions along the vertical and horizontal trajectories of the spray droplets.

After the spray droplet stains were collected on the chromatography papers, the papers each measuring 50cm x 40cm were cut into 5cm x 4cm units giving a total of 100 units. The stain sizes were placed under a microscope fitted with eyepiece micrometer for size or diameter measurement.

The chromatography paper has at its back water sensors connected to an alarm system. The alarm system indicates the time at which the water droplets touched the chromatography papers. For each cloud of spray droplets, 30 droplets were sized. At the end of the experiments, measurements such as the time-distance or flights-time, droplet initial diameter, droplet velocity, wind speed, wet and dry bulb temperatures, barometric pressures, droplet final diameter, etc were made. The experiments were carried out at two air conditions of still air and varying air velocity of 1.0 m/s.

3. RESULTS AND DISCUSSION

The results of the numerical computations and experimental validation tests are presented in Figures 1-4 and Tables 1-2. Figure 1 presents the comparison of the results of the simulation and validation experiments at still air condition. It indicates that 10 seconds after leaving the sprayer nozzle, the simulation predicted a size reduction range of 100 to 88.40 microns, while the experiment recorded a size reduction range of 100 to 92.00 microns. The trend is noticeable in the other droplet sizes of 150, 200 and 250 microns.

Figure 2 illustrates the comparison of the droplet size reductions as obtained from simulation and experiment at the wind velocity of 1.0 m/s. It is observed that droplet size reduction was generally higher at the wind velocity of 1.0 m/s than at the still air condition. Also, droplet size decreases as the air-borne time increases thereby increasing the rate of change of the spray droplet sizes. The observation is true for all the spray droplet sizes used for the validation experiments and was in line with similar studies (Miller and Hadfield 1989; Law and Bowen, 1975).

The two Figures (1&2) compare the droplet size reductions at still air and windy field conditions. The comparison indicates that droplet size reduction increased significantly as wind velocity increased from 0 m/s to 1.0 m/s. This could be explained using the kinetic theory of molecular diffusion. It is well known that liquids contain molecules which are in constant random motion. Each of these molecules moves at different random velocities. In a non-convective evaporation process, the diffusion of liquid molecules away from the droplet surface controls the the mass transfer rate of the droplets. At the surface of the liquid droplets, some molecules with sufficient kinetic energy may break through the liquid surface and encounter some molecules of air or vapor and as such may be forced to fall back to the droplet surface after the collision. When wind blows, the molecules of the air or vapor surrounding the droplet surface will be removed, clearing the way for the liquid molecules breaking through the surface of the droplet liquids. The faster the wind blows, the faster will be the rate of movement of the liquid molecules out of the droplet surface. Hence the faster will be the rate of evaporation of the liquid droplet sizes.

In the case of still air, the diffusion and random motion of the liquid molecules control the rate of loss of weight of the droplet. The absence of wind reduces the rate of removal of the air or vapor molecules surrounding the droplet surface. Therefore, the liquid molecules at the droplet surface will continue to collide with the molecules of air or vapor and hence forced to fall back to the liquid droplet surface with random velocities. The random collision of the molecules and their different random velocities caused the non- linear pattern of the percentage reduction in the sizes of the droplets at still air as shown in Figures 3 and 4.

Figures 3 and 4 compare the percentage size reductions of the simulated and experimental results at still air and wind velocity of 1.0 m/s respectively. Figure 3 indicates that at sill air, a 100 microns droplet size recorded a size reduction of 8% for the experimental results and 11.60 % for the simulated results. It is observed from Figure 3 that percentage size reduction increased as the droplet size decreased. For instance, the 100 microns recorded 8 % size reduction, while the 250 microns recorded 4.32 % reduction during the experimental validation tests. The result is in agreement with similar studies by Williamson and Threadgill (1974) Goering et al, (1972). The same trend holds for the simulated results, with a size decrease of 11.6 % for 100 microns and 7.78 % for 250 microns droplet sizes.

The reason for the observed increase in percentage size reduction as the droplet size decreases is based on the understanding that droplet size reduction due to evaporation is essentially a surface phenomenon, which depends on the ratio of surface area to volume. This ratio is low for large droplet sizes and high for small droplet sizes. The higher the value of the ratio, the higher the increase in percent size reduction and the lower the value of the ratio, the lower the percent size reduction.

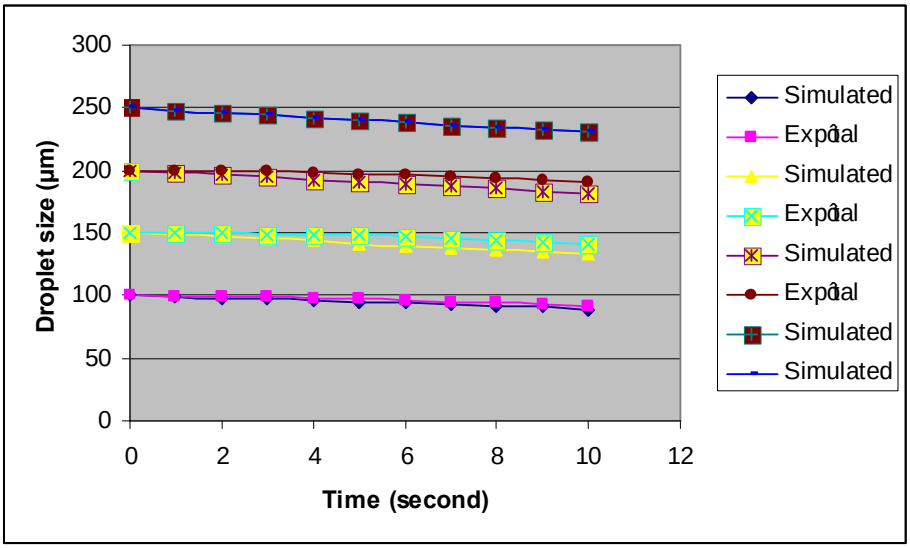


Fig.1: Comparison of droplet size reduction of simulated and experimental results at still air.

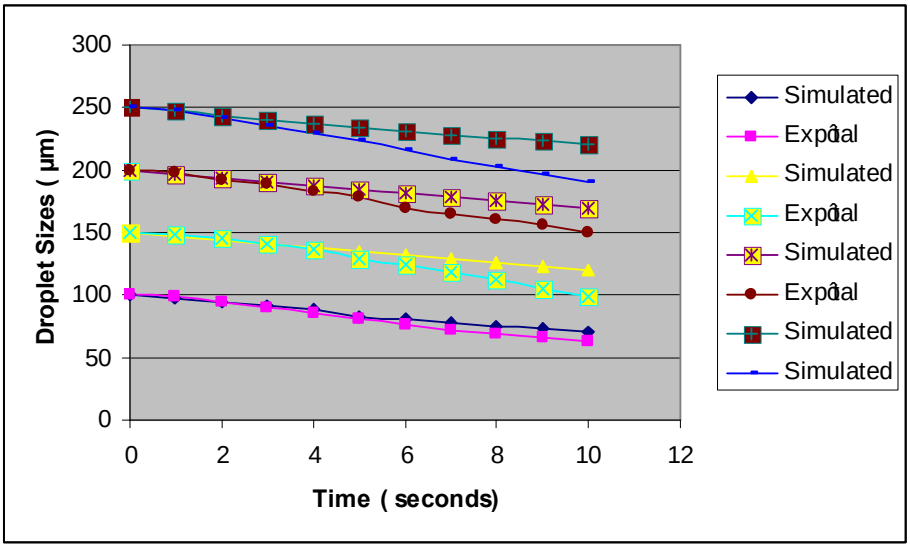


Fig.2: Comparison of droplet size reduction of simulated and experimental results at the wind velocity of 1.0m/s.

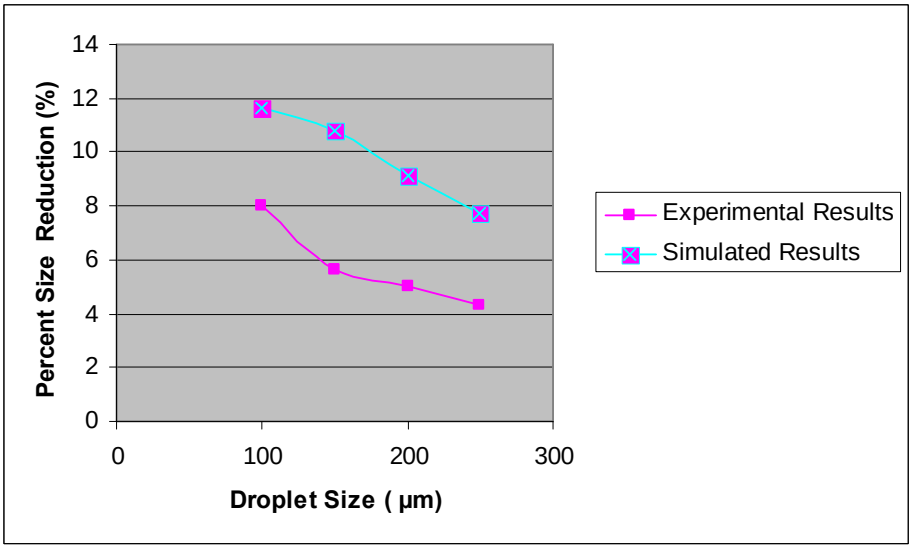


Fig.3: Percentage droplet size reduction of the simulated and experimental results at still air

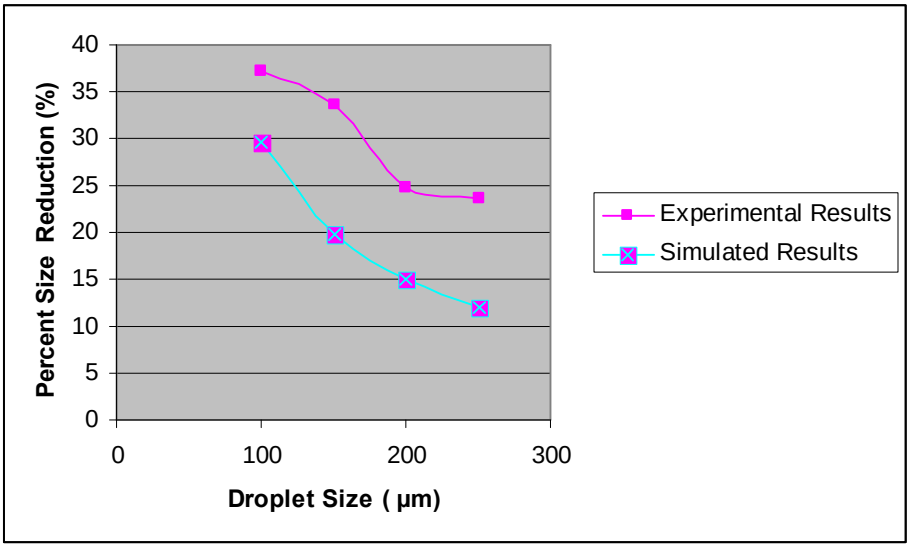


Fig. 4: Percentage droplet size reduction of the simulated and experimental results at wind velocity of 1.0 m/s.

Table 1: Range of droplet size reduction and percentage deviation of the simulated results from the experimental results at still air.

Original droplet size (microns)	Size reduction range for Experimental results(microns)	Size reduction range for Simulated results(microns)	Deviation of simulated results from Expâtal results (%)
100	100-92.00	100-88.40	3.60
150	150-141.50	150-133.83	5.12
200	200-190.00	200-181.81	4.09
250	250-239.20	250-230.55	3.46

Table 2: Range of droplet size reduction and percentage deviation of simulated results from the experimental results at the wind velocity of 1.0 m/s.

Original droplet size (microns)	Size reduction range for Experimental results (microns)	Size reduction range for Simulated results(microns)	Deviation of simulated results from Expâtal results (%)
100	100-62.80	100-70.48	7.68
150	150-99.48	150-120.20	13.82
200	200-150.25	200-170.01	9.88
250	250-191.20	250-219.88	11.48

With the percentage deviation range of 3.60-5.12 % for 100-250 microns respectively (Table 1) at still air and 7.68-11.48 for 100-250 microns respectively (Table 2) at the wind velocity of 1.0m/s, the simulated and experimental results compare fairly well. The comparison of the percentage droplet size reductions of the simulation and experimental results at the wind velocity of 1.0 m/s(Figure 4) reveals that droplet size reductions were higher for the experimental results than the simulated results. The experimental results recorded a 37.2 % size reduction for 100 microns and 23.52 % size reduction for 250 microns. In the case of the simulated results, 29.525 and 12.04 % size reductions were predicted for the 100 microns and 250 microns respectively.

The difference between the values of the experimental and simulation results is attributed to the intrinsic properties of air-vapor mixtures whereby the water molecules present in any air-vapor mixtures exert pressures on the surroundings and do not exactly follow the perfect gas laws (Singh and Heldman, 2005). However, the models were developed to follow the gas laws. Generally, when Figure 4 and 2 are compared with Figures 1 and 3, there is the indication that the model actually described and predicted size reduction of spray droplets at still air condition and at the wind velocity of 1.0 m/s. The good agreement of the simulated and experimental results justifies the inclusion of the latent heat of vaporization of the liquid droplets and the thermal conductivity of the transport medium (air) as important parameters in predicting air-borne size reduction phenomenon in liquid spray droplets. This should be so especially in a tropical environment where the ambient air temperature could be as high as 40 ^{o}C at certain periods of the year.

4. CONCLUSIONS

From the simulated and experimental results, the following conclusions were deduced:

At still air, the developed model predicted a percentage size decrease of 11.6, 10.78, 9.09 and 7.758 % for droplet sizes of 100, 150, 200 and 250 microns respectively after 10 seconds of being air-borne. The percent deviations of simulated results from validation results were 3.6, 5.12, 4.09 and 3.46 % for the droplet sizes of 100, 150, 200, 250 microns respectively.

In the case of windy environment at the wind speed of 1.0 m/s, the model predicted a percentage size reduction of 29.52, 19.86, 14.99 and 12.04 % for the droplet sizes of 100, 150, 200, and 250 microns respectively after 10 seconds of leaving the sprayer nozzle.

The percent deviation of simulated results from validation results indicates 7.68, 13.82, 9.88, and 11.48 % for the droplet sizes of 100, 150, 200, and 250 microns respectively

Under still air condition, small liquid droplets have longer air-borne time or retention time in air than the large ones. The longer the retention time, the more the evaporation rate which leads to decrease in droplet size and hence, the more chances of off-target deposition.

The size reduction of an air-borne spray droplet increases as the droplet retention time in air increase. This means that the distance between the spray nozzle and the target should be as small as possible to reduce the air-borne time. Wind velocity affects the evaporation of air-borne liquid droplets. The higher the wind velocity, the higher the rate at which droplet sizes decrease, implying that spraying at windy environment should be discouraged.

REERENCES

Braig, M. B. 1986. A numerical simulation of the disposal of liquids from aircraft. Transactions of ASAE. 29 (1) 10-15.

Goering, C. E.; Bode, L. E. and Gebhardt, M. R. 1972. Mathematical Modeling of spray droplet deceleration and evaporation. Transactions of the ASAE, 15 (1), 220-225.

Law, S. E. and Bowen, H. D. 1975. Theoretically predicted Interaction of surface charge and evaporation of air borne pesticide droplets. Transactions. 18 (1), 35-45.

Marshall, W. R. 1955. Heat and mass Transfer in spray drying. Transactions, 77: 1377-1385.

Marchant, J. A. 1977. Calculation of spray droplet Trajectory in a moving air stream. Journal of Agricultural Engineering Research. Vol. 22, pp. 93-96.

Miller, P. C. H. and Hadfield, D. J. 1989. A simulation model of the spray drifts from hydraulic nozzles. Journal of Agricultural Engineering Research. 42, 135-147.

Ranz, W. E. and Marshall, W. R. 1952. Evaporation from Drops, part I & II. Chemical Engineering Progress. 48 (3) 141-146 & 48 (4) 173-180.

Singh, R. P. and Heldman, D. R. 2005. Introduction to Food Engineering. Food Science and Technology, International Series, Third Edition. Academic Press. Pp. 473-495.

Smith, D. B; Harris, F. D. and Butler, B.J 1982. Shielded Sprayer Boom to reduce Drift. Transactions. 25 (2), 1136-1141

Sutton, O. G. 1953. Micrometeorology. McGraw-Hill Book Company, New York.

Williamson, R. E. and Threadgill, E. D. 1974. A simulation for the Dynamics of Evaporating Spray drops in Agricultural spraying. Transactions, 17 (1), 254-261.